https://doi.org/10.5194/egusphere-2023-2438
Preprint. Discussion started: 9 January 2024

First measurements of ecosystem-scale biogenic volatile organic compound fluxes over rapeseed reveal more significant terpenoid emissions than expected

Pauline Buysse[1,2], Benjamin Loubet[1], Raluca Ciuraru[1], Florence Lafouge[1], Brigitte Durand[1], Olivier Zurfluh[1], Céline Décuq[1], Olivier Fanucci[1], Lais Gonzaga-Gomez[1], Jean-Christophe Gueudet[1], Sandy Bsaibes[3], Nora Zannoni[3,4], Valérie Gros[3]

[1]INRAE-AgroParisTech, Université Paris Saclay, UMR ECOSYS, Palaiseau, 91120, France
[2]now at INRAE-Institut Agro, UMR SAS, Rennes, 35000, France
[3]UMR CNRS-CEA-UVSQ, Université Paris Saclay, IPSL, LSCE, Gif-sur-Yvette, 91190, France
[4]now at Institute of Atmospheric Sciences and Climate, National Research Council, Bologna, 40129, Italy
Correspondence to: Pauline Buysse (pauline.buysse@inrae.fr)

Abstract. Biogenic volatile organic compounds (BVOCs) play a large role in atmospheric chemistry as they are precursors of ozone and secondary organic aerosols. However, the analysis of their emission in croplands is scarce. This work constitutes, to our knowledge, the first quantification of ecosystem-scale biogenic volatile organic compounds (BVOC) fluxes exchanged over a rapeseed crop field. The experimental campaign took place at the FR-Gri ICOS site (near Paris, France) between spring and summer 2017, during which the BVOC fluxes were measured continuously by the eddy-covariance method with a proton-transfer quad-injection time-of-flight mass-spectrometer instrument (PTR-Qi-TOF-MS). Standard emission factors (SEF) and OH reactivity fluxes were computed from the measured fluxes, and compared to the widely used model MEGAN2.1. Fifty-three BVOCs were significantly emitted or deposited during the campaign. Methanol was by far the most emitted one (83 to 91 % of summed emissions), followed by ethanol (1.5 to 11 %) and monoterpenes (1.2 to 1.6 %). Methanol SEF appeared to be overestimated during vegetation stages in MEGAN2.1. In addition, a 4-fold increase of emissions during the late senescence stage confirmed the necessity to use the ageing factor to represent methanol emissions in MEGAN2.1. Most noticeably, monoterpenes SEF computed in this study were 3 to 90 times larger than with MEGAN2.1. Consequently, this study shows that the share of OH reactivity represented by terpenoid compounds was underestimated in previous studies, pointing out the potentially more significant contribution of croplands to secondary organic aerosol formation.

1 Introduction

Volatile organic compounds (VOCs) only make up a small fraction of air composition and are negligible greenhouse gases, but they play an important role in atmospheric chemistry and have an indirect effect on climate (Isaksen et al., 2009; Peñuelas and Staudt, 2010). Indeed, in the presence of nitrogen oxides and solar radiation, these compounds can form ozone, a greenhouse gas and pollutant (Atkinson and Arey, 2003; Sartelet et al., 2012). They are also precursors of secondary organic aerosols (SOA) when influenced by solar radiation and meteorological parameters like temperature and humidity (Mahilang et al., 2021; Sakulyanontvittaya et al., 2008). Also, by reducing the oxidative capacity of the atmosphere through the consumption of OH radicals, they can increase methane lifetime in the troposphere (Kaplan et al., 2006; Stevenson et al., 2020).

VOC emissions can be either anthropogenic or biogenic (BVOCs), the latter representing 90 % of the total emissions (Guenther et al., 1995) globally. According to Karl et al. (2009), forests contribute 55 % of total BVOC emissions from terrestrial

https://doi.org/10.5194/egusphere-2023-2438
Preprint. Discussion started: 9 January 2024

ecosystems and agricultural lands to 27 % in Europe. Forests are strong emitters of the two most contributing BVOC species, isoprene and monoterpenes (Sindelarova et al., 2014), while croplands mostly release oxygenated BVOCs like methanol and acetone (Bachy et al., 2016, 2018, 2020; Das et al., 2003; Gonzaga Gomez et al., 2019; Graus et al., 2013; Havermann et al., 2022; Loubet et al., 2022; Wiß et al., 2017). As forests are the largest emitters of terpenoids globally (reactive compounds that significantly impact atmospheric chemistry), forests have been more studied than agricultural ecosystems. However, better quantification of BVOC exchanged fluxes in agricultural ecosystems is needed and started a decade ago. The variety of crop species and phenological stages have to be considered and documented to improve regional and global BVOC emission estimates, as they greatly influence the type and magnitude of BVOC emissions (Courtois et al., 2009; Manco et al., 2021; Vivaldo et al., 2017). For example, the MEGAN2.1 model (Guenther et al., 2012) gathers all crop species into a unique "crop" category so that BVOC emission factors reflect neither the variety among crop species nor the phenological stages of the crops.

Among the main crop species in Europe, wheat and maize are the crop species in which BVOC emissions have been the most widely quantified from the leaf to the ecosystem scale and through laboratory experiments (Mozaffar et al., 2018; Piesik et al., 2011) and field campaigns (Bachy et al., 2016, 2020; Gallagher et al., 2000; Gonzaga Gomez et al., 2019; Morrison et al., 2016). However, although rapeseed represents a large share of oilseed production in France, Europe, and the world, data on BVOC emissions from rapeseed plants and fields are scarce. France is indeed the first country in Europe in rapeseed production. Europe is the world leader (30 %) in this crop production (Woźniak et al., 2019), with rapeseed representing the most significant share of oilseed production (63 %) in Europe and the second most important one after soya bean in the world (FAOSTAT, 2023). Early VOC studies performed on rapeseed, using adsorption on Tenax-TA tubes and subsequent gas chromatography-mass spectrometry (GC-MS) analysis, provided qualitative VOC-emitted profiles (Butcher et al., 1994, 1995) and relative concentration profiles (Konig, 1995; Mcewan and Macfarlane Smith, 1998). The former reported the emission of oxygenated BVOCs, together with terpenoid-like compounds, and the latter showed that flowering rapeseed was emitting various types of terpenes, together with a few sulphur compounds. Later, Müller et al. (2002), using the cuvette technique, adsorption on sampling tubes and subsequent GC-MS analysis, quantified emission fluxes of monoterpenes, together with some carbonyl compounds. They also pointed out the significant difference between the fluxes measured in earlier studies and their work, likely attributed to differences in measurement techniques. Havermann et al. (2022) recently performed direct chamber measurements on rapeseed plants in the field and reported emission fluxes for 25 BVOCs using a proton transfer reaction quadrupole mass spectrometer (PTR-QMS 500).

However, to our knowledge, quantification of BVOC fluxes in rapeseed crops at the field scale is missing. Recent developments in the measurement techniques of VOCs, such as the PTR-Qi-TOF-MS, now allow measuring the concentration of a wide range of BVOCs down to the ppt level (Sulzer et al., 2014). When integrated with an eddy-covariance setup, it becomes possible to quantify an extensive range of BVOC fluxes continuously at the field scale (Loubet et al., 2022). It has the advantage of quantifying net emission and deposition fluxes in actual conditions (no disturbance due to chambers) integrated over several hectares (generally from about 4 ha up to 60 to 70 ha in forested areas). The objectives of this study were i) to identify the main exchanged BVOCs from a rapeseed field at the different stages of crop development, ii) to quantify BVOC fluxes (emission and deposition) at the field scale using the eddy-covariance technique, iii) to provide emission factors specific to rapeseed, therefore contributing to improve modelled BVOC emissions in croplands, and iv) to evaluate the potential effect of these emissions on OH reactivity in the atmosphere, relative to existing emission factors.

https://doi.org/10.5194/egusphere-2023-2438
Preprint. Discussion started: 9 January 2024

2 Material and Methods

2.1 Measurement site

The field campaign occurred at the Grignon FR-Gri site, about 40 km west of Paris (France). The site is part of the European ICOS network (Integrated Carbon Observing System, www.icos-ri.eu). It consists of a 19-ha field on a relatively flat plateau with a gentle slope of approximately 1 % towards the northeast. The site is surrounded by other agricultural fields and a farm with animal houses to the southwest (at around 400 m distance). The farm is substantial, with about 200 cows and 500 sheep and a production of 900 lambs per year on average. As shown by earlier studies at the same site (Kammer et al., 2020; Loubet et al., 2011, 2022), this farm is a large source of ammonia and a significant source of VOCs, among which methanol, ethanol and acetaldehyde, together with trimethylamine and dimethylsulfide. The field is also bordered by a road with heavy traffic located at more than 900 m to the east and other roads with less traffic to the north (300 m) and west (700 m), which were shown to be sources of NO_x (Vuolo et al., 2017). Loubet et al. (2011) give more details about the site.

The field is managed with the following crop rotation: maize, winter wheat, winter barley, and mustard as a catch crop, and with reduced tillage since 2000. Rapeseed (*Brassica napus* L.) is also sown occasionally at the field site, such as in August 2012 and 16 August 2016 (Bohême variety) for the present field campaign. The field usually receives a variable amount of nitrogen ranging between 150 and 300 kg N ha^{-1} y^{-1}, mainly as nitrogen solution and cattle manure (usually once every 3 years; the last application was on 12 August 2016). Before the present campaign, the field received 3 times 39 kg N ha^{-1} as a liquid solution of NH_4NO_3 (20 February, 3 March and 22 March), two insecticide applications (12 and 28 March, 0.05 l ha^{-1}, MAGEOS®) and a fungicide application (15 April, 0.4 l ha^{-1}, FILAN SC®). The preceding crop was winter wheat, harvested in July 2016. Rapeseed was harvested on 30 July 2017.

2.2 Eddy-covariance BVOC fluxes

BVOC fluxes were measured continuously from 7 April to 25 August 2017 with the eddy-covariance (EC) method. The setup was similar to the one in Loubet et al. (2022). Air was sampled at 2.7 m height and drawn through a 50 m heated PTFE tube with a pump working at a 50 L min^{-1} flow rate (SV-1010, Busch, Switzerland). The three components of the wind velocity (u, v, w) and the sonic temperature were recorded at 20 Hz with an ultrasonic anemometer (model R3-50, Gill Instruments Ltd., UK), 20 cm apart from the air inlet.

BVOC concentrations were measured at 10 Hz with a Proton Transfer Reaction Quadrupole ion, Time-Of-Flight, Mass Spectrometer (PTR-Qi-TOF-MS, Ionicon, Innsbruck, Austria), operated at the same conditions as in Gonzaga Gomez et al. (2019). In the drift tube, the pressure P_d was set to 4 ± 0.01 mbar, the drift temperature T_d to 80 ± 0.06 °C, and the drift voltage E to 995 ± 0.03 V, while the extraction voltage at the end of the tube U_{Dx} was 44 ± 0.20 V. These conditions ensured an E/N ratio (where N is the number density of the gas molecules in the drift tube) of 132 ± 0.03 Td (1 Td = 10^{-17} V cm^{-2}). Once extracted from the drift tube, the protonated ions were pulsed and separated according to their mass-to-charge (m/z) ratio at a rate of 25 kHz, leading to 2500-extracted spectra per 100 ms. The detection channels were set to 240 000, and the mass spectrum spanned from m/z 15 to m/z 530.

The raw data (in counts per second, cps) from the PTR-Qi-TOF-MS were acquired with Labview software to synchronize the output from the Tofdaq software with the ultrasonic anemometer data at 20 Hz. Files containing 5 min of synchronized data were stored for post-computation. Mixing ratios for each VOC i (C_i) were computed following the same procedure as the one described in Loubet et al. (2022). The uncalibrated mixing ratio of the compound $C_{i,ptr}$ (ppb) was calculated as Eq. (1):

https://doi.org/10.5194/egusphere-2023-2438
Preprint. Discussion started: 9 January 2024

$$C_{i,ptr} = 1.657e^{-11} \times \frac{U_{drift} T_{drift}^2}{k\, p_{drift}^2} \times \frac{cps_{R_iH^+}^{trans}}{cps_{H_3O^+}^{trans} + cps_{H_2O \cdot H_3O^+}^{trans}} \quad (1)$$

$$cps_{R_iH^+}^{trans} = \frac{TR_{H_3O^+}}{TR_{R_iH^+}} \times cps_{R_iH^+} \quad (2)$$

where U_{drift} is the voltage of the drift tube (V), T_{drift} is the drift tube temperature in kelvin (K), cps_{RiH+} is the cps of the production *i*, cps_{H3O+} and $cps_{H2O \cdot H3O+}$ are the cps of the ion source and the first water cluster, k is the proton transfer reaction rate assumed to be constant for all compounds (2.5×10^{-9} cm^3 s^{-1}), *trans* stands for normalized transmission, TR_{H3O+} is the transmission factor for H_3O^+, TR_{RiH+} is the transmission factor for the product ion i, and p_{drift} is the pressure in the drift (mbar). The transmission curve from the supplier was used to compute the transmission. $cps_{H_3O^+}^{trans}$ was computed from ion m/z 21.022 ($H_3^{18}O^+$) by multiplying by the isotopic factor of O^{18} / O^{16} in water (487.56), taking the first water cluster as the ion peak m/z 37.028. The constant $1.657e^{-11}$ was derived from the PTR-Qi-TOF-MS setup.

The calibrated mixing ratio C_i was then computed by subtracting the zero-air concentration $C_{i,ptr}^{zero\ air}$ and multiplying by a calibration coefficient S_i, similarly as in Gonzaga Gomez et al. (2019):

$$C_i = S \times \left(C_{i,ptr} - C_{i,ptr}^{zero-air}\right) \quad (3)$$

The calibration coefficient S_i was computed as the slope of the regression (with intercept forced to zero) between $C_{i,ptr}$ and the prescribed mixing ratio of toluene during calibrations. Calibrations were performed almost every week, based on the use of a standard cylinder containing 102 ppbv of benzene, 104 ppbv of toluene, 130 ppbv of ethylbenzene and 336 ppbv of xylene (122 ppbv Ortho, 121 ppbv Meta, 123 ppbv Para; BTEX, Messer). Gas from this cylinder was diluted with synthetic air (alphagaz 1, Air Liquide, France) using a fluorinert coated mass flow controller (Bronkhorst). The calibration factor *S* was calculated based on m/z 93 only and applied to all compounds as explained and discussed in Gonzaga Gomez et al. (2019); S was equal to 4.87 ± 0.24 on 3 April and decreased to 2.47 ± 0.02 on 4 May, after which it remained pretty constant (2.46 ± 0.03 on 16 August). The background mixing ratio $C_{i,ptr}^{zero-air}$ was determined every 30 minutes by passing the sampled air through a hydrocarbon filter (Supelco ref 22445-12) for 2 minutes and using the value obtained from the integration of the signal during the last 30 seconds. Further details on the calibration procedure can be found in (Loubet et al., 2022).

The BVOC eddy covariance flux was computed based on standard eddy-covariance procedures following Loubet et al. (2022):

$$F_i = \frac{\overline{p_a^d}}{R\overline{T_a}} \overline{w' C_i'} \quad (4)$$

Where F_i is the flux (nmol m^{-2} s^{-1}), *w* is the vertical wind component, $\overline{T_a}$ is the air temperature (K), $\overline{p_a^d}$ is the dry air pressure (Pa), and *R* is the ideal gas constant (8.31 J mol^{-1} K^{-1}). Overbars ($\bar{}$) denote averages, and primes denote fluctuations around the mean following Reynolds decomposition rules. Here w' was calculated by applying two rotations following Aubinet et al. (2000). The covariance between C_i' and w' was calculated after dephasing the two signals with a lag time τ computed as the time at which the correlation function $\overline{w'(t) \chi_{i,}\, d'\,(t-\tau)}$ was the largest in absolute value (Langford et al., 2015). The time lag changed during the field campaign due to a decreased flow rate following the mast displacement during crop management operations. The time lag was 3.55 s before harvest and 4.95 s after harvest. The time lag did not differ between a selection of VOC compounds and was therefore set equal for all BVOC compounds.

The random uncertainty on the flux (RU_i) was calculated as the standard deviation over a 10 s period of the covariance function $corr_{w'C_i'}(t)$ around $t = 80s$ and $t = -80s$ as described by Spirig et al. (2005). The mean hourly fluxes ($\overline{F_i}^h$) and random

https://doi.org/10.5194/egusphere-2023-2438
Preprint. Discussion started: 9 January 2024

uncertainty $\overline{RUi}^h$ were computed based on the 5-min data. The flux was averaged, but the random uncertainty was computed using a quadratic mean (Langford et al., 2015) as:

$$\overline{RUi}^{\mathrm{h}} = \frac{1}{N}\sqrt{\sum_{i=1}^{N} RUi^2} \quad (5)$$

Where N is the number of 5-min periods in an hour, which was 8 or below since 20 min per hour was dedicated to profile and calibration measurements.

High-frequency losses were evaluated to be below 5 % by Loubet et al. (2002) and were therefore neglected. A footprint analysis (ICOS report, 2021) showed that 80 % of the total footprint contribution was always within the studied area.

2.3 Ancillary data

Meteorological measurements were performed continuously at the FR-Gri site during the campaign following the ICOS standards. Among other variables, air temperature (Tair) and air humidity (RH) (HMP155a, VAISALA, Finland) at 1, 2.7 and 5 m heights, global incoming short-wave solar radiation at 5.3 m (model CNR4, Kipp & Zonen, Germany), and rainfall (model ARG100, Campbell, UK) were recorded.

CO_2 and H_2O fluxes were measured by eddy-covariance following the ICOS protocol (www.icos-ri.eu) using an enclosed path infrared gas analyser (model Li-7200, Li-COR, USA) and an ultrasonic anemometer (model HS-50, Gill Instruments Ltd, UK), located at around 50 m away from the BVOC mast. Crop height evolution was monitored at regular intervals. The leaf area index (LAI) and above-ground biomass were determined on three dates (11 November 2016, 16 March 2017 and 19 April 2017) with destructive samplings and planimeter measurements. The LAI was 5.2 ± 1.5 $m^2_{leaf}\, m^{-2}_{soil}$ during the experiment (rapeseed plants were at their maximum leaf development when the experiment started), of which 80 % were leaves, and 20 % stems.

2.4 Flux data treatment and analysis

2.4.1 Focus on four specific periods

To determine the effect of vegetation development stages on BVOC fluxes, the data analysis was focused on four 1-week periods representing contrasted vegetation development stages (BBCH stages, (AHDB, 2023)): P1 (15 to 22 May), the start of fruit development phase (BBCH stages 70s); P2 (10 to 17 June), the start of the senescence phase (BBCH stages 80s); P3 (30 June to 7 July), the end of the senescence phase (BBCH stages 90s); and P4 (10 to 17 August), bare soil (actually soil with rapeseed residues on the ground), as rapeseed was harvested on 30 July. Using a moving window, we verified that each of these selected weeks represented each targeted vegetation period based on the net CO_2 fluxes and provided that sufficient data was available.

2.4.2 Selection of compounds with significant fluxes

For each studied period, only the BVOCs with mean fluxes larger than three times the random uncertainty were considered significant and selected for further analyses in this work. We computed the 7-day running means of $\overline{F_i}^h$ ($\overline{F_i}^{7d}$) and $\overline{RUi}^{\mathrm{h}}$ ($\overline{RUi}^{7d}$) using the same quadratic averaging as in eq. (5) for $\overline{RUi}^{\mathrm{h}}$. By using moving windows, it was possible to detect singularities in the dataset. For each moving 7-day window, the BVOC selected were those for which $\overline{F_i}^{7d} > 3 \times \overline{RUi}^{7d}$.

2.4.3 Other compounds selection and uncertainties in the identification

In addition, iron-containing compounds identified as artefacts by Gonzaga Gomez et al. (2019) were withdrawn from the list of compounds. Furthermore, the detected BVOC with a peak at m/z 63.006 could not be wholly distinguished from the m/z peak at

https://doi.org/10.5194/egusphere-2023-2438
Preprint. Discussion started: 9 January 2024

63.026 during the campaign; the identification of this compound is therefore uncertain: it could be dimethylsulfide (DMS) instead of methaneperoxoic acid.

2.4.4 Calculation of Standard Emission Factors

As BVOC emissions by vegetation are driven by both temperature and light or solely by temperature, these emissions can be normalised by light and temperature functions to produce standardised emission factors (SEF), which are helpful for comparison with previous studies. The SEF were calculated based on Guenther et al. (1995, 1997) as described by Gonzaga Gomez et al. (2019). For fluxes depending on light and temperature, such as isoprene, the SEF E_{S_i} (µg m^{-2} h^{-1}) is defined by:

$$E_{S_i} = \frac{E_i}{C_L\, C_T} \quad (6)$$

Where E_i is the BVOC flux per leaf surface (µg m^{-2} h^{-1}), and C_L and C_T are the temperature and light response function of the BVOC emissions, defined as:

$$C_T = \frac{\exp\left[\frac{C_{T1}(T-T_S)}{R\,T_S\,T}\right]}{1+\exp\left[\frac{C_{T2}(T-T_M)}{R\,T_S\,T}\right]}, \qquad C_L = \frac{\alpha\, C_{L1}\, L}{\sqrt{1+\alpha^2 L^2}} \quad (7)$$

Where C_{T1} = 95000 J mol^{-1}, C_{T2} = 230000 J mol^{-1}, T_M = 314 K, α = 0.0027, C_{L1} = 1.066 are empirically derived constants, T is the leaf experimental temperature (K), T_S is the leaf temperature at standard condition (303 K), R the gas law constant (8.314 1 J mol^{-1} K^{-1}), and L is the photosynthetically active radiation (PAR) flux (µmol photon m^{-2} s^{-1}).

For fluxes depending only on temperature (e.g. monoterpenes), the SEF is defined using the following equation with the empirical constant β set to 0.09 K^{-1}:

$$Es_i = \frac{E_i}{\exp(\beta(T-T_S))\exp(\beta(T-T_S))} \quad (8)$$

To compute the SEF, the BVOC emission per leaf surface, E_i (µg m^{-2} h^{-1}), was computed from the molar flux $\overline{F_t}^{7d}$ (nmol m^{-2} s^{-1}), the molar mass M_i (g mol^{-1}) of compound i, and the leaf area index (LAI, m^2 m^{-2}) as:

$$E_i = \frac{3600}{1000} \times \frac{M_i}{LAI} \times \overline{F_t}^{7d} \quad (9)$$

Where the ratio 3600/1000 converts seconds to hours and ng to µg. It should be noticed that the SEF computed in this study represent the ecosystem and not the plants alone since the eddy-covariance fluxes integrate over the whole ecosystem.

The SEF calculated for all the compounds showing a significant emission for each of the four periods were compared to values taken from three references: i) the MEGAN2.1 model (Guenther et al., 2012), ii) the study by Havermann et al. (2022) and iii) the study by Gonzaga Gomez et al. (2019):

- MEGAN2.1 is a widely used model that provides estimates of BVOC flux exchanges between the terrestrial biosphere and the atmosphere. This model categorises ecosystems between 15 plant functional types (PFT) and does not distinguish between crop species as they all fall into a unique category (PFT 15). Additionally, bare soil is considered to have null BVOC emissions. The model also categorises BVOCs into individual (e.g. methanol, isoprene, acetone) and compound classes (bidirectional VOC, stress VOC, etc.) according to chemical characteristics. Although we did not strictly use the same model as MEGAN2.1 to compute the SEF from the measured fluxes, the equations are comparable in Guenther et al. (1995) and MEGAN2.1.
- Havermann et al. (2022) measured BVOC flux using large chambers deployed on three crop species (maize, rapeseed and ryegrass). They then calculated the SEF based on empirical light- and temperature-dependent relationships. Since they report SEF on a dry weight basis, we divided their SEF by the leaf specific area for rapeseed they report (39.6 m^2 kg^{-1}) to retrieve the

https://doi.org/10.5194/egusphere-2023-2438
Preprint. Discussion started: 9 January 2024

SEF per unit leaf area. It has to be noted that the leaf specific area measured in the present study is 20 ± 1 m^2 kg^{-1}, which is half of what is reported by Havermann et al. (2022).

- Gonzaga Gomez et al. (2019) measured BVOC fluxes using dynamic automated chambers deployed on rapeseed, wheat and maize at the same site and field campaign as the one reported in the present study. They calculated the SEF based on the empirical light- and temperature-dependent relationships from Guenther et al. (1995).

2.4.5 Calculation of the OH reactivity flux

The OH reactivity R (s^{-1}) is usually calculated as (Gros and Zannoni, 2022):

$$R = \sum_i k_{OH+i} \times N_{avo} \times \frac{P}{R \times T} \times 10^{-15} \times C_i \quad (10)$$

Where k_{OH+i} (cm^3 $molecule^{-1}$ s^{-1}) is the rate constant of the reaction between OH and VOC *i* (Table 2 and references therein), N_{avo} (6.022 10^{23} molecule mol^{-1}) is the Avogadro number, P (101325 Pa) is the atmospheric pressure, R (8.314 J/(K mol^{-1})) is the gas law constant, T (298 K) is the air temperature, 10^{-15} is a conversion factor, and C_i (nmol mol^{-1}) is the concentration of VOC *i*.

To compare the OH reactivity resulting from the SEF found in this study to those resulting from literature emission factors, we computed a standard OH reactivity flux (here indicated as RF). It is representative of a net OH reactivity that would result from the emitted VOC. It was computed as:

$$RF = \sum_i k_{OH+i} \times N_{avo} \times \frac{P}{R \times T} \times 10^{-15} \times \left(SEF_i \times V_{mol}^{air} \times \frac{LAI}{M_i} \times \frac{1000}{3600}\right) \quad (11)$$

Where SEF_i is the standard emission factor of VOC *i*, and the term on the right side of the equation is needed to transform the SEF unit into nmol mol^{-1} m s^{-1}, which leads to RF being in m s^{-2}, that is the unit of the OH reactivity (s^{-1}) multiplied by an exchange velocity (m s^{-1}). V_{mol}^{air} (m^3 mol^{-1}) is the air molar volume, M_i (g mol^{-1}) is the molar mass of VOC i and LAI is the leaf area index (m^2 m^{-2}).

In this study, we used the OH reactivity flux to compare the impact of VOC SEF computed here with the SEF available from the model MEGAN 2.1. To do that, only the compounds with a SEF explicitly reported in MEGAN 2.1 were used in this calculation.

3 Results

3.1 Meteorological conditions and crop development

The BVOC flux measurement campaign started as rapeseed was already in the fruit development phase (P1) and actively photosynthesising, as shown by the Net Ecosystem Exchange (NEE) fluxes being largely negative during daytime. This period, which was also characterised by significant evaporation, corresponded to the end of the flowering period, as confirmed by the albedo being lower in April when the bright yellow flowers were fully developed. In the second period (P2; start of senescence), an apparent decrease in the CO_2 flux was observed while evaporation was sustained. The P3 period showed a cut in photosynthesis with a positive NEE and reduced evaporation, indicating that the crop was completely senescent. The latest period occurred after harvest (P4, bare soil), which was carried out on 30 July, as can be seen by the disturbance of the albedo during that period. Average air temperatures during the four periods were 15.4, 18.7, 19.2 and 17.8 °C, being, therefore, the highest in P2 and P3 (Fig. 1). The average above-ground rapeseed biomass sampled and determined at the maturity stage was 781 ± 188 g m^{-2}.

https://doi.org/10.5194/egusphere-2023-2438
Preprint. Discussion started: 9 January 2024

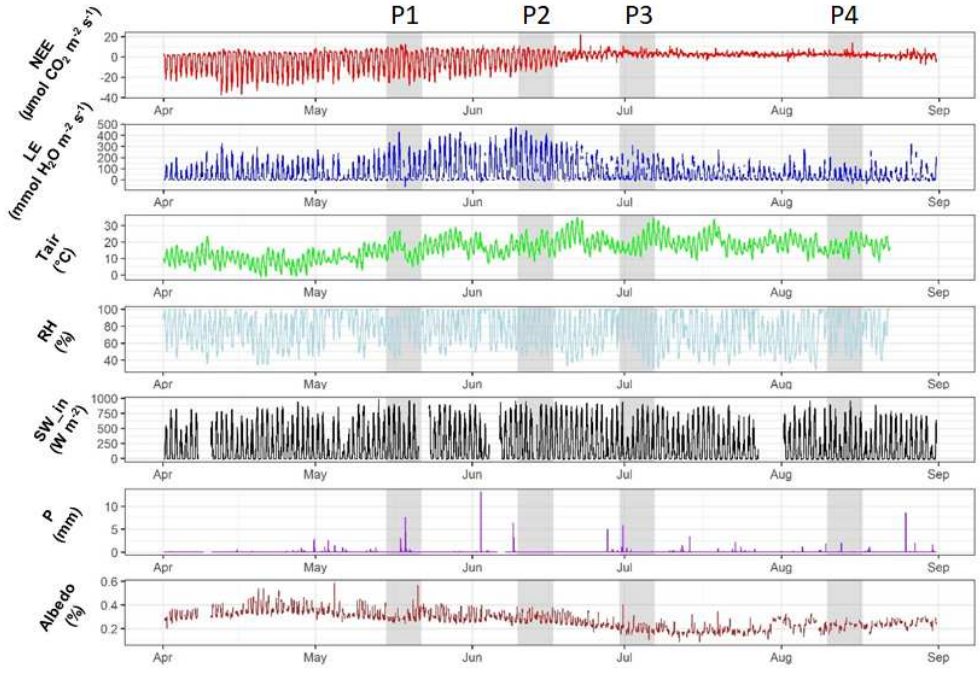

Figure 1: CO_2, H_2O fluxes and meteorological conditions during the field campaign: net ecosystem exchange (NEE [µmol CO_2 m^{-2} s^{-1}]), latent heat (LE [mmol H_2O m^{-2} s^{-1}]), air temperature (T_{air} [°C]), relative humidity (RH [%]), short-wave incoming radiation (SW_in [W m^{-2}]), precipitation (P [mm]) and Albedo (%). The four grey-shaded periods represent periods P1, P2, P3 and P4, successively. Rapeseed harvest was carried out on 30 July.

3.2 Exchanged BVOCs

Fifty-three BVOCs exhibited significant emission or deposition fluxes over the four periods of focus (see Table 1 for details about the twenty compounds showing the most significant fluxes and the Supplementary Material S01 for the complete list of compounds with details on their emission and deposition). Fig. 2 provides a quick look at the twenty most exchanged compounds and their evolution over the four investigated periods. Most compounds were emitted, and only ten were deposited. Not all the detected compounds could be identified; most BVOCs were identified based on our knowledge and the GLOVOC database (Yáñez-Serrano et al., 2021).

Among the emitted BVOCs, methanol (m/z 33.033) was by far the most important one for all four periods (Fig. 2), representing between 83 and 91% of the total emissions on a molar basis (Table 1). The magnitude of methanol emissions was about three times larger during the end of the senescence phase (maximum of about 15 nmol m^{-2} s^{-1} during the day) than during the fruit development and bare soil phases (maximum of about 5 nmol m^{-2} s^{-1} during the day) (Fig. 3). The second most emitted compound was ethanol (m/z 47.048, with contributions of 6.9, 1.5 and 11 % of total emissions in P2, P3, and P4, respectively), followed by monoterpenes (m/z 137.129, 1.2 to 1.6% of emissions) and acetone (m/z 59.049, 1.1 to 1.5% of emissions) when the crop was present. Contrarily to methanol, acetone and monoterpenes were not detected on bare soil. Formic acid (m/z 47.013) and acetic acid (m/z 61.029) were the most deposited compounds, with about 79 % and 53 %, and 16 % and 26 % of total depositions during senescence phases (P2 and P3), respectively. Formic acid was also deposited during the fruit development phase (P1), but this was not significantly different from zero (Table 1), while acetic acid was emitted during that period. Surprisingly, BVOCs were only emitted during the bare soil period (P4), as none of the detected compounds was seen to deposit.

Table 1: Twenty most emitted and deposited compounds during the four periods. Average air temperature (Ta_mean, [°C]) and incoming total radiation (Rg_mean, [W m^{-2}]) are mentioned for each period. The proportions (Prop., (%)) of emissions/depositions for each compound with respect to the total fluxes are indicated separately for each period (in this table, the total for both net emitters and net depositers does not reach precisely 100 %, as this was established based on the 53 detected compounds (see the complete list in Appendix). The flux uncertainty values between brackets represent the root square of the squared difference to the mean.

				Period 1 15 May - 22 May End of the flowering period		Period 2 10 June - 17 June Start of senescent period		Period 3 30 June - 7 July End of senescent period		Period 4 10 August - 17 August Bare soil	
			Net Emitted / Deposited	Ta_mean = 15.4 °C	Rg_mean = 225.7 W m^{-2}	Ta_mean = 18.7 °C	Rg_mean = 289.1 W m^{-2}	Ta_mean = 19.2 °C	Rg_mean = 214.9 W m^{-2}	Ta_mean = 17.8 °C	Rg_mean = 188.7 W m^{-2}
m/z	**Molecular formula**	**Tentative compound name**	**E or D**	**Prop.[c] (%)**	**Mean Flux (nmol m^{-2} s^{-1})**	**Prop. (%)**	**Mean Flux (nmol m^{-2} s^{-1})**	**Prop. (%)**	**Mean Flux (nmol m^{-2} s^{-1})**	**Prop. (%)**	**Mean Flux (nmol m^{-2} s^{-1})**
31.018	(CH2O)H+	Formaldehyde	E		ns		ns	9.2	0.657 *(1.165)*[d]		ns
33.033	(CH4O)H+	Methanol	E	90.7	2.577 *(0.0486)*	85.3	2.550 *(0.0294)*	84.5	5.969 *(0.0215)*	83.2	1.856 *(0.0175)*
45.033	(C2H4O)H+	Acetaldehyde	E		ns		ns	0.6	0.041 *(0.0024)*	2.6	0.057 *(0.002)*
47.048	(C2H6O)H+	Ethanol	E		ns	6.9	0.208 *(0.0003)*	1.5	0.111 *(0.0002)*	11.1	0.248 *(0.0001)*
49.014	(CH4S)H+	Methanethiol	E	0.5	0.015 *(0.0003)*	0.8	0.022 *(0.0003)*	0.6	0.042 *(0.0002)*	0.6	0.013 *(0.0002)*
57.033	(C3H4O)H+	Propanoyl	E		ns	0.2	0.007 *(0.0037)*	0.2	0.014 *(0.0026)*	0.4	0.009 *(0.002)*
59.049	(C3H6O)H+	Acetone	E	1.5	0.043 *(0.0005)*	1.3	0.039 *(0.0003)*	1.1	0.079 *(0.0002)*		ns
63.006	(CH2O3)H+	Methaneperoxoic acid	E		ns	0.6	0.019 *(0.0001)*	0.3	0.022*	0.5	0.012*
69.07	(C5H8)H+	Isoprene	E	0.3	0.010 *(0.0003)*	0.3	0.009 *(0.0002)*	0.2	0.014 *(0.0001)*	0.3	0.006 *(0.0001)*
81.068	(C6H8)H+	Monoterpene or sesquiterpene fragment	E	1.0	0.029 *(0.0002)*	0.7	0.022 *(0.0001)*	0.2	0.012 *(0.0001)*		ns
137.129	(C10H16)H+	Monoterpenes	E	1.6	0.045 *(0.0003)*	1.2	0.036 *(0.0002)*		ns		ns
61.029	(C2H4O2)H+	Acetic acid	E or D	0.7	0.021 *(0.0002)*	15.8	-0.018 *(0.0001)*	25.6	-0.031 *(0.0001)*	0.5	0.010 *(0.0001)*
47.013	(CH2O2)H+	Formic acid	D	100.0	-0.042 *(0.067)*	78.7	-0.090 *(0.0463)*	52.7	-0.064 *(0.0367)*		ns
71.048	(C4H6O)H+	MACR / MVK	D		ns	4.0	-0.005 *(0.0008)*		ns		ns
99.008	(C4H2O3)H+	Maleic anhydride	D		ns	1.6	-0.002 *(0.0005)*	1.8	-0.002 *(0.0004)*		ns
223.057	(C11H10O5)H+	*not identified*	D		ns		ns	6.9	-0.008*		ns
224.058	(C11H10O5)H+	isotope of m223.057	D		ns		ns	1.4	-0.002*		ns
225.036	(C14H8O3)H+	*not identified*	D		ns		ns	7.0	-0.008*		ns
226.038	(C13H7NO3)H+	2-Nitro-9-fluorenone	D		ns		ns	1.3	-0.002*		ns
227.022	(C13H6O4)H+	*not identified*	D		ns		ns	2.6	-0.003*		ns

a Net emitter (E) or depositer (D) characteristic is evaluated over each period. D/E denotes that this BVOC was seen to behave both as a net emitter and a depositer over all 4 periods. b Based on the GLOVOC database. c Proportions were calculated within each net deposited or emitted group of compounds for each respective period. d Error is calculated as the root of the sum of squares of data over each respective period. (*) Error is lower than 0.0001. "ns" denotes that the measured flux was not significant during that given period for that given BVOC.

https://doi.org/10.5194/egusphere-2023-2438
Preprint. Discussion started: 9 January 2024

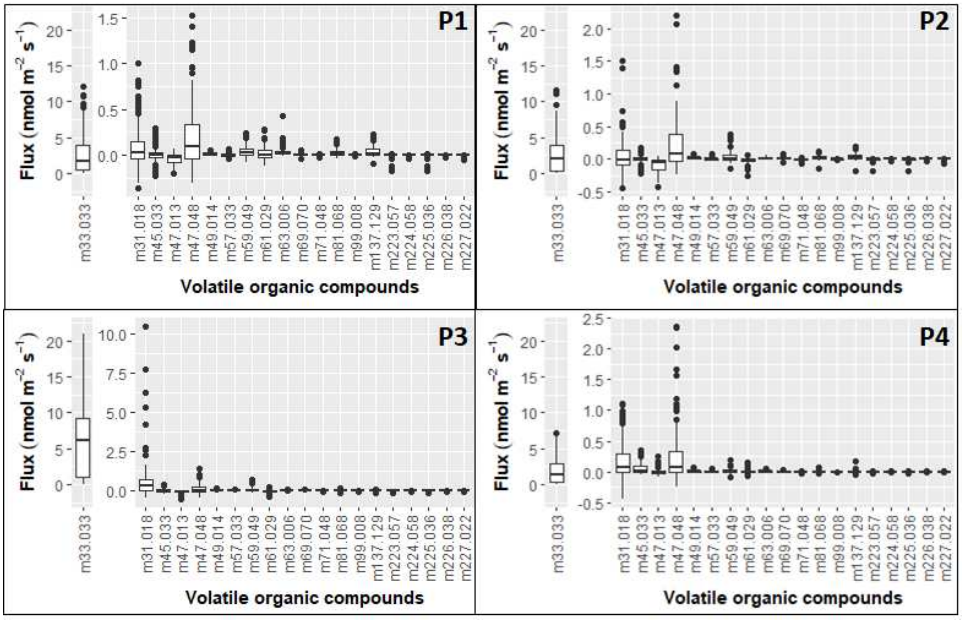

Figure 2: Boxplots representing the emission and deposition fluxes of the twenty most exchanged BVOCs during the four investigation periods. Note the different y-axis for methanol (m/z 33.033).

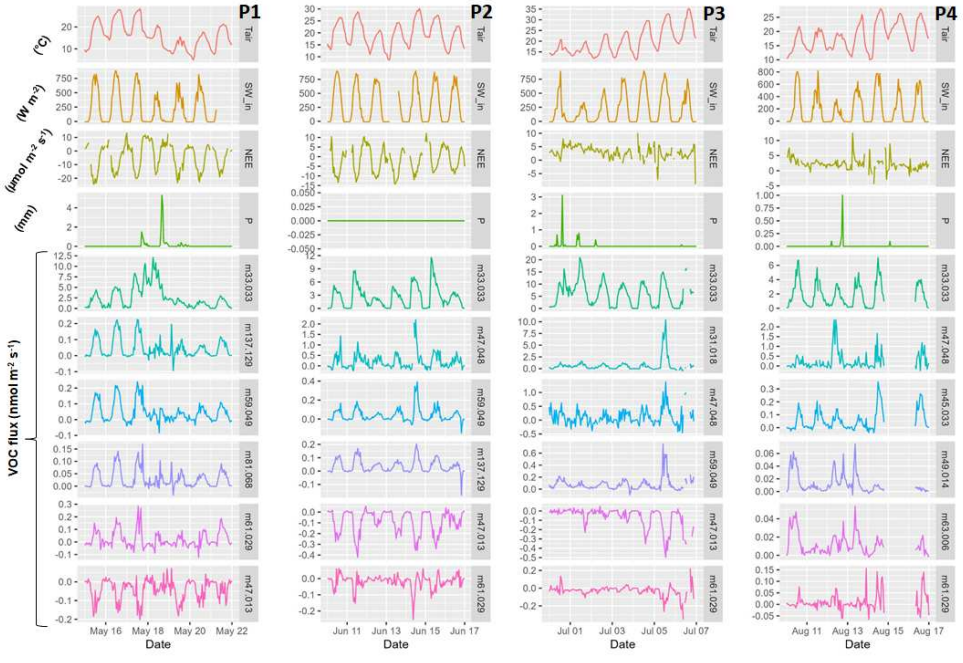

Figure 3: Air temperature (T_{air} [°C]), short wave incoming radiation (SW_in [W m^{-2}]), net ecosystem exchange (NEE, [µmol CO_2 m^{-2} s^{-1}]), Precipitation (P [mm]), and exchanged fluxes (nmol m^{-2} s^{-1}) of a selection of 4 most emitted and 2 most deposited BVOCs over the four crop development periods. BVOCs are named from their m/z ratio. P1 represents the fruit development period, P2 the start of senescence, P3 the end of the senescence and P4 the bare soil after harvest.

https://doi.org/10.5194/egusphere-2023-2438
Preprint. Discussion started: 9 January 2024

Some compounds were emitted in lower quantities and more sporadically during the four periods, like formaldehyde (m/z 31.018, 9 % of emissions in P3), acetaldehyde (m/z 45.033, respectively 0.6 and 2.6 % of emissions in P3 and P4), methanethiol (m/z 49.014, emitted in small amounts 0.5-0.8% of emissions during all four periods) and isoprene (m/z 69.070, emitted in tiny amounts, 0.2-0.3 % of emissions, during all four periods).

Interestingly, one BVOC, acetic acid (m/z 61.029), was either emitted at low rates (average of about 0.02 nmol m^{-2} s^{-1}) during the fruit development phase (P1) and over bare soil (P4) or deposited at similarly close absolute rates during both senescence phases P2 and P3.

All the detected compounds exhibited diel emission or deposition patterns during all four periods of interest (Fig. 3 for some BVOCs of interest). BVOC fluxes increased (in absolute value) during the day and decreased to lower nocturnal emission rates following radiation and temperature variations. During P1, a rain event occurred on the 17th and 18th of May (Fig. 1), and a temperature drop likely caused reductions in all the detected BVOC emission rates (Fig. 3). Formic acid deposition rates did not increase. The short rain events during P3 and P4 did not decrease BVOC emissions, probably because rain intensity was smaller than in P1 and air temperatures remained high. During P3, a temperature increase that started in the middle of the week, together with bright sun conditions until the end of the week, could have triggered slightly larger methanol emissions (m/z 33.033) during the second half of the week. In contrast, emissions of formaldehyde (m/z 31.018), ethanol (m/z 47.048) and acetone (m/z 59.049) only peaked on 5 July (data gaps on 6 July prevent having a clear view of what happens on 6 July). During that period, more significant deposition rates of formic (m/z 47.013) and acetic (m/z 61.029) acids were also observed. These more significant deposition rates could result from larger concentrations of these two compounds at that time (Fig. 4).

A closer look at mixing ratios and deposition velocities (Vd = – Flux/Mixing ratio) for methanol and the main net depositing compounds (m/z 47.013, 61.029, 71.048 and 99.008) is brought in Fig. 4. It shows that mixing ratio levels were smaller in P4 for all these compounds as compared to the other three periods. Mixing ratios likely increase at the end of P3 as a response to increased air temperature. Positive deposition velocities, denoting deposition processes being at work, are always observed during vegetated periods for formic acid (m/z 47.013), while deposition velocities for acetic acid (m/z 61.029) are negative in P1 and P4 and very slightly positive in P2 and P3. Besides, Vd values for methanol are always negative (both during day and night), showing that this species is never deposited during the four periods.

https://doi.org/10.5194/egusphere-2023-2438
Preprint. Discussion started: 9 January 2024

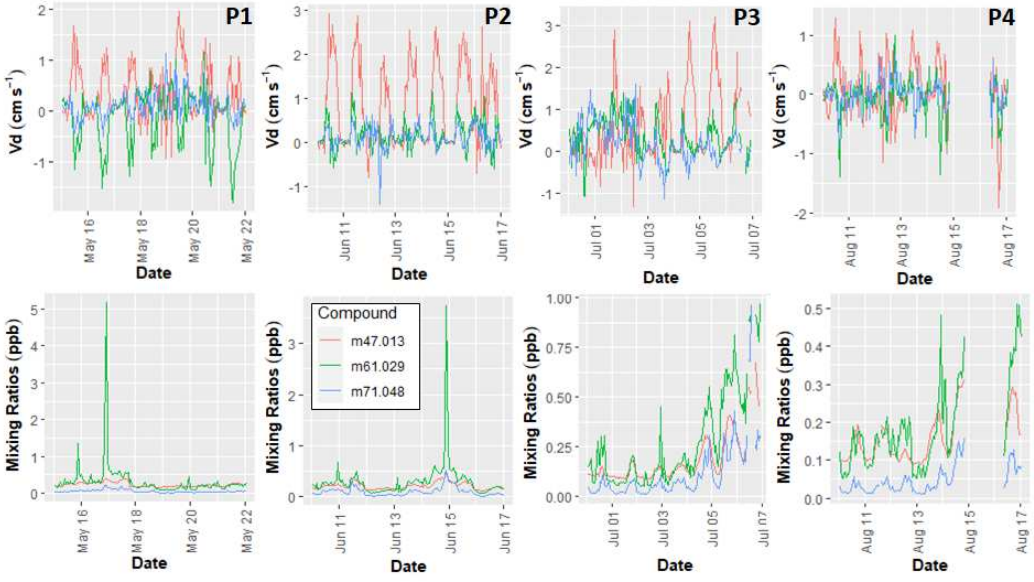

315

Figure 4: Deposition velocities (Vd (cm s^{-1})) and mixing ratios (ppb) for the three main net depositing compounds (m/z 47.013, 61.029 and 71.048) during each of the four periods.

During some periods, a few compounds exhibited a maximum flux during the morning, followed by a decrease during the rest of the day (Fig. 5, panels A, B and C). This was the case for methanol (m/z 33.033) emissions during P1 and P2, for
320 formic acid (m/z 47.013) deposition during P2 and P3 and the emissions of acetic acid (m/z 61.029) and m/z 63.006 during P4. During P1, NEE flux and radiation also peaked earlier than noon (Fig. 5, panels D and E), while this was not the case in the last three periods. Fig. 5B also shows small deposition fluxes of acetic acid (in P1) and ethanol (during P2 and P3) in the morning (before sunrise).

https://doi.org/10.5194/egusphere-2023-2438
Preprint. Discussion started: 9 January 2024

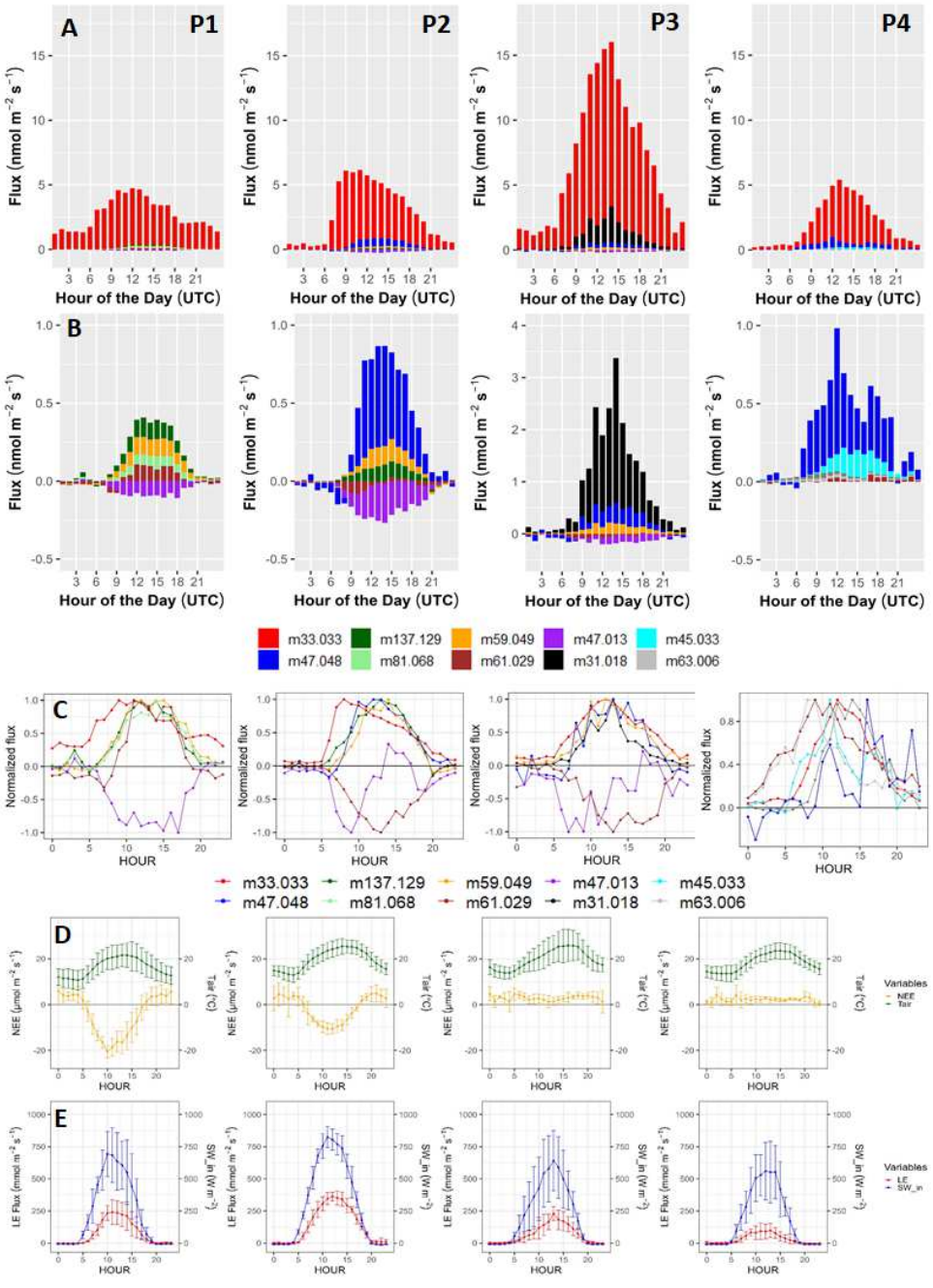

Figure 5: Details of diel hourly cycles of main BVOC fluxes and micro-meteorological variables during the four periods: A, stacked hourly BVOC fluxes (nmol m^{-2} s^{-1}) for 8 most emitted and 2 most deposited BVOCs (corresponding colours for m/z compounds are given below graph B); B, same graph as A, without methanol (m/z 33.033); C, normalised BVOC fluxes (BVOC fluxes divided by the maximum flux for each respective BVOC); D, net CO_2 fluxes (NEE, [µmol CO_2 m^{-2} s^{-1}]) and Air temperature (T_{air}, [°C]); E, latent heat fluxes (LE, [mmol H_2O m^{-2} s^{-1}]) and global incoming radiation (SW_in, [W m^{-2}]).

https://doi.org/10.5194/egusphere-2023-2438
Preprint. Discussion started: 9 January 2024

3.3 Emission factors and OH reactivity fluxes

The calculated standard emission factors (SEF) showed much larger values for methanol than for other oxygenated BVOCs like acetone, ethanol, acetaldehyde, and for terpenoid compounds (isoprene, monoterpenes, MBO, sesquiterpenes) (Table 2). Concerning the vegetated periods (P1, P2 and P3), the largest SEF observed in this study corresponded to methanol emissions during the end of the senescence period (P3) and was about 4 times larger than during P1 and P2. When the soil was bare, the SEF values calculated for P4 cannot be compared with other SEF values expressed per m^2 of leaf.

Compared to values taken into consideration in the MEGAN2.1 model (Guenther et al., 2012), and concerning compounds having been the most discussed in the literature, the SEF calculated in the present study exhibit values

- about 3.5 to 4 times smaller for methanol in P1 and P2, but similar values for P3
- about 5 to 6 times smaller for acetone in P1 and P2, and about 3.5 times smaller in P3
- about 3 (P1-P2) to 7 (P3) and 9 (P4) times larger for isoprene
- between 3.5 and 90 times larger for monoterpenes (P1 and P2)
- of the same order of magnitude for sesquiterpenes and formaldehyde (P1)
- much smaller for indole, n-hexenal (two compounds that are not part of the twenty most exchanged compounds (Table 1), but which were significantly detected during P1 (indole) or P3 (n-hexenal) and are part of the 53-significant-compound list, see Supplementary Material), methanethiol and 4-oxopentanal
- and of the opposite sign for formic acid (P1-P3).

Compared to the studies by Gonzaga Gomez et al. (2019) and Havermann et al. (2022), the values reported in the present study are closer to their order of magnitude, even if

- less than twice larger for methanol in P1 and P2
- about 2 (P3 and P4) to 5 (P1 and P2) times smaller for isoprene
- and about 1.5 to 2 times larger for monoterpenes in P1 and P2.

In this study, the OH reactivity fluxes (RF) were about twice lower for methanol, ethanol and acetic acid, four times larger for isoprene, six times lower for acetaldehyde and nine times larger for monoterpenes, as compared to values based on MEGAN2.1 SEF values. Other main compounds had roughly comparable values. However, given the much larger SEF for n-hexenal, indole, methanethiol and 4-oxopentanal reported in MEGAN2.1, the corresponding RF values are much larger (350 to 500 times) for these compounds, as compared to what we calculated in the present study. In order not to introduce a large disequilibrium, we therefore chose not to include these compounds in the evaluations of the total OH reactivity flux and the contributions of each compound to this total amount. In terms of BVOC contribution to the total OH reactivity flux, monoterpenes dominate and contribute 4 times more than with MEGAN2.1 values, for which contributions are mainly shared in the same range (17-34 %) by monoterpenes, sesquiterpenes and acetaldehyde. In our study, the contribution of methanol to total OH reactivity flux is also seen to be three times less than what is evaluated with MEGAN2.1 values.

Table 2: Standard emission factors (SEF) calculated in the present study for the four crop development periods, compared with the values from the previous studies, either obtained from experimental or modelling works. P1 represents the end of flowering and fruit development, P2 is the start of senescence, P3 is the end of senescence, and P4 is the bare soil after harvest. The values appearing in column H2022 were calculated based on emission rates (SEF) reported by Havermann et al. (2022).

			Standard emission factor (SEF) µg m^{-2} (leaf) h^{-1}							OH reactivity constant (k_{OH+i}) cm^3 $molecule^{-1}$ s^{-1}	OH reactivity flux (RF) $m\,s^{-2}$		Contribution to total OH reactivity %	
			This study				MEGAN2.1[b]	G2019[c]	H2022[d]		This study	MEGAN2.1	This study	MEGAN2.1
m/z	Ion formulas	VOC names	P1	P2	P3	P4					P1-P3		P1-P3	
Oxygenated and terpenes VOC[e]														
33.033	(CH4O)H+	methanol	252	245	1114	2009	900	na	150	9×10^{-13} (c)	12.7	21.3	2.84 %	1.13 %
59.049	(C3H6O)H+	acetone	11.8	9.1	26.1	na	80	na	11	1.8×10^{-13} (c)	0.1	0.7	0.03 %	0.02 %
69.07	(C5H8)H+	isoprene	3.0	2.3	6.9	9.0	1	12-18	11	1×10^{-10} (c)	22.4	5.5	4.99 %	0.14 %
87.08	(C5H10O)H+	MBO	2	na	na	2	0.01	na	na					
137.129	(C10H16)H+	monoterpenes	28	18	na	na	0.3 - 5	9-23	14	1.24×10^{-10} (c)	309	35.8	68.99 %	0.34 %
205.13	(C15H24)H+	sesquiterpenes	3	na	na	na	2-4	na	na	1.5×10^{-10} (c)	74.7	73.6	16.69 %	0.63 %
Bi-directional VOC														
31.018	(CH2O)H+	formaldehyde	na	na	86	na	80	na	na	8.5×10^{-12} (c)	18	16.8	4.02 %	0.95 %
45.033	(C2H4O)H+	acetaldehyde	na	na	13.1	77	80	na	5.5	1.5×10^{-11} (c)	7.1	43.1	1.58 %	1.67 %
47.013	(CH2O2)H+	formic acid	-7.0	-14.1	-6.5	na	80	na	na	4.5×10^{-13} (@)	-0.2	1.3	-0.03 %	0.05 %
47.048	(C2H6O)H+	ethanol	na	36	29	175	80	na	22	3.2×10^{-12} (c)	3.9	9.6	0.87 %	0.36 %
61.029	(C2H4O2)H+	acetic acid	8.6	-2.7	1.5	11.0	80	na	41	6.9×10^{-13} (@)	0.1	2.7	0.02 %	0.08 %
Stress VOC														
99.078	(C6H10O)H+	n-hexenal	na	na	0.6	na	300	na	na	4.76×10^{-11} (*)	2.2	1127.6	na	na
118.065	(C8H7N)H+	indole	0.8	na	na	na	300	na	na	1.54×10^{-10} (*)	12.1	4347.3	na	na
Other VOC leaf surface compounds														
49.011	(CH4S)H+	methanethiol	2.1	2.9	10.5	15	140	na	na	3.3×10^{-11} (@)	6.6	180.5	na	na
101.06	(C5H8O2)H+	4-oxopentanal (4-OPA)	2.3	1.3	2.3	na	140	na	na	2×10^{-11} (§)	3.2	225.5	na	na
										Summed reactivity flux[f]	447.9	210.4	100 %	100 %

a SEF calculated with the equation proposed by (Guenther et al., 1995; Guenther, 1997), depending on both temperature and radiation. Note: For P4, it is expressed as m^{-2}(soil). b Values from Guenther et al. (2012). c Values from Gomez et al. (2021). d Values from Havermann et al. (2022), considering a rapeseed biomass density of 1100 g m^{-2} and a leaf specific area of 39.6 m^2 kg^{-1}. e Categories from MEGAN2.1 model (Guenther et al. (2012). f summed reactivity not accounting for "stress VOC" and "other VOC leaf surface compounds". (@) Values from IUPAC standard reference base (https://iupac-aeris.ipsl.fr/). (*) Values from Atkinson et al. (1995). ($) Value from Fruekilde et al. (1998). "na" means that no data were available.

https://doi.org/10.5194/egusphere-2023-2438
Preprint. Discussion started: 9 January 2024

4 Discussion

4.1 Nature of BVOCs exchanged during the field campaign

4.1.1 New references for plot-scale BVOC exchanges in a rapeseed crop

To our knowledge, this is the first study presenting eddy-covariance BVOC fluxes from a rapeseed crop. This technique has already been applied to maize and wheat fields (Bachy et al., 2016, 2018, 2020; Karl et al., 2001; Loubet et al., 2022) and in forest ecosystems (Brilli et al., 2016; Gallagher et al., 2000; Park et al., 2013, 2014), where it is successful in providing BVOC flux estimates at the plot scale, integrating both the soil and the vegetation. Compared to chamber measurements, eddy-covariance also allows (i) to detect more reactive species given the shorter residence time in the inlet tube than in chambers, and (ii) to quantify deposition fluxes, mainly because turbulence is larger in the field than in the air circulating through a chamber, and also because some chambers are sometimes filled with zero air.

4.1.2 Domination of methanol in net emissions

In the present study over a rapeseed crop, methanol was found to have the largest fluxes of all measured BVOCs, and its contribution varied between 83 and 91 % of the summed BVOC emitted fluxes on a molar basis. The dominant methanol contribution observed in this work agrees with the previous studies by Gonzaga Gomez et al. (2019) and Havermann et al. (2022), both performed using automated dynamic chambers deployed on rapeseed plants in the field. The study by Gonzaga Gomez et al. (2019), carried out at the same field site as the present study but using two cuvettes containing one plant each, showed a methanol contribution of 56 to 77 % of the summed BVOC emissions, while Havermann et al. (2022) reported a contribution of more than 80 %. Other studies performed at the field scale and in chambers enclosing other crop species also pointed out methanol as the dominant BVOC emitted from crops and from grasslands (for maize, see Bachy et al. (2016), Das et al. (2003), Graus et al. (2013), Wiß et al. (2017); for winter wheat see Bachy et al. (2018), 2020, Gonzaga Gomez et al. (2019), Loubet et al. (2022); for grasslands see Ruuskanen et al. (2011)).

The methanol emissions observed in this study, ranging between about 0.1 and 16 nmol m^{-2} s^{-1}, are larger than those reported by Bachy et al. (2016, 2018, 2020), obtained by the eddy-covariance method for maize and wheat crops, as the methanol fluxes were between about 250 and 350 (in absolute values) µg m^{-2} h^{-1} (= 2.1 to 3 nmol m^{-2} s^{-1}) in these studies.

However, Methanol emissions were smaller than the value of 37.5 to 39 nmol m^{-2} s^{-1} reported by Gonzaga-Gomez et al. (2019) after converting their units and considering a measured plant biomass of 780 g m^{-2} at maturity. A difference is expected because of the higher temperature in the chambers. Scaling to the soil temperature would lead to a better agreement between Eddy Covariance and Chambers (see *Appendix K* in Gonzaga Gomez et al. (2019)).

4.1.3 Other emitted oxygenated and non-oxygenated BVOCs

The present study reported the observation of significant exchanged fluxes of other oxygenated BVOCs like acetaldehyde (m/z 45.033), acetone (m/z 59.049) and acetic acid (m/z 61.029), which were also reported by other studies performed in croplands using continuous flux measurements with dynamic chambers (Gonzaga Gomez et al., 2019; Havermann et al., 2022), eddy-covariance method (Bachy et al., 2016, 2018, 2020) and GC analysis after adsorption on cartridges (Veromann et al., 2013), with different flux magnitudes between the studies. In the present study, acetone was the third most emitted compound during all three periods with rapeseed cover. Das et al. (2003) and Graus et al. (2013) observed acetone as

https://doi.org/10.5194/egusphere-2023-2438
Preprint. Discussion started: 9 January 2024

maize's second most important emitted BVOC. Bachy et al. (2016) observed bidirectional fluxes of acetone in maize. Bachy et al. (2020) also observed acetone emissions in wheat's late crop-stage development (ear development and senescence).

Other oxygenated compounds like formaldehyde (m/z 31.018) and ethanol (m/z 47.048) emitted during our field campaign do not appear in all the above-listed studies. However, formaldehyde fluxes should be considered with caution due to uncertainties in its response to air humidity (Loubet et al., 2022). However, Brilli et al. (2016) observed these two compounds in an eddy-covariance measurement campaign performed in a poplar plantation.

Other BVOCs like m/z 57.033 (acrolein), 73.064 (methyl-ethyl-ketone (MEK) or ethyl-vinyl-ether), 83.084 (green leaf volatiles (GLV) fragments), 85.064 (ethyl-vinyl-ketone), 87.042 (butanoic acid) were emitted in smaller but significant quantities during vegetation stages and to a lesser extent over bare soil (Table 1 for m/z 57.033 and Table S01 in Supplementary material for other compounds). MEK and GLV were also reported by Brilli et al. (2016) and Havermann et al. (2022).

4.1.4 Terpenoid BVOCs

Emissions of terpenoid compounds, including isoprene (m/z 69.070), monoterpenes (m/z 137.129) and sesquiterpenes (m/z 205.186), were also observed in the present study. Previous works by Butcher et al. (1994, 1995) and Jakobsen et al. (1994) during different rapeseed flowering stages reported terpenes emissions from measurements of BVOC with sampling on Tenax TA tubes followed by analysis with gas chromatography. More recently, Havermann et al. (2022) reported emissions of terpenoids like monoterpenes, sesquiterpenes and oxygenated monoterpenes from chamber measurements enclosing rapeseed biomass. However, terpenoid compounds were emitted in smaller quantities than oxygenated compounds.

4.1.5 Deposited BVOCs

Much fewer BVOCs were deposited in the present study than those observed in winter wheat fields (Bachy et al., 2020; Loubet et al., 2022). Indeed, out of the BVOCs seen to be deposited in Loubet et al. (2022), only formic acid (m/z 47.013) and acetic acid (m/z 61.029) exhibited similar behaviour in the present study, the latter showing bi-directional fluxes. Deposition fluxes of acetic acid (m/z 61.029) were reported by Bachy et al. (2020) over a winter wheat crop (from emergence until the second stage of plant senescence) and by Bachy et al. (2016) over bare soil. In the case of the present study, deposition of this compound was mainly observed during the senescence stages. At the same time, at the end of the fruit development period, it was seen to have a bi-directional behaviour, with minimal deposition fluxes before sunrise and significant emissions during the day. It was also seen to be emitted on bare soil. Mixing ratios of acetic acid were in the same range in all four periods, which is not likely to explain why it was deposited mainly during senescence stages and less or not during the other periods. Kesselmeier et al. (1998) demonstrated that uptakes of acetic and formic acids in crop plants were related to stomatal exchange. The observations for both acids in the present study are, therefore, primarily consistent with the observations of Kesselmeier et al. (1998) performed with corn, pea, barley and oat (but not rapeseed), except for the fruit development period, when acetic acid emissions were primarily reported. Gomez et al. (2021), however, showed that acetic acid switched from deposition to emission fluxes when the plant entered senescence, which is opposite to what was observed in the present study at the ecosystem level, as deposition fluxes of acetic acid were observed during P2 and P3. This suggests that during the senescence stages, as the plant parts get degraded, acetic acid may be released from the plant but would then be deposited on the soil or elsewhere within the whole crop canopy.

Differences with observations by Loubet et al. (2022) also relate to GLV fragments (m/z 83.049) and 4-Oxopentanal (m/z 101.059), which were emitted in the present study but deposited in their study over a winter wheat field. Besides, hydroxyacetone (m/z 75.044) and ion m/z 43.018 did not show a significant flux both over rapeseed and bare soil, contrary

https://doi.org/10.5194/egusphere-2023-2438
Preprint. Discussion started: 9 January 2024

to Loubet et al. (2022), who found a deposition flux around one-third of the methanol emission. Besides, formaldehyde (m/z 31.018) was emitted at the end of the rapeseed senescence stage. At the same time, this compound exhibited large deposition fluxes at the beginning of the wheat field campaign in Loubet et al. (2022), then decreased progressively to near zero emissions at the end of the observation period. Also, while deposition fluxes of methanol at night were observed in winter wheat fields (Bachy et al., 2020; Loubet et al., 2022), this was not the case in the present work, as the fluxes remained slightly above zero overnight. Finally, the heavier compounds (m/z 223.057, 224.058, 225.036, 226.038, 227.022 and 229.005) showing small deposition fluxes in the present study were not reported in these two studies. In contrast, only BVOCs of m/z 223.057 and 225.036 were seen to be deposited in small amounts by Gonzaga Gomez et al. (2019) in chambers placed on rapeseed plants, either at night or in the early morning.

The observation of few deposited compounds and small deposition fluxes in the present study could be explained by two hypotheses. First, relatively small mixing ratios could prevent the compounds from deposition on the soil and crop surfaces, particularly at night. At least for methanol, average mixing ratios tended to be slightly lower (0.95 ± 0.92 ppb) than values reported for this same compound in a winter wheat field at the same site (3.4 [1-10] ppb (Loubet et al., 2022)). However, mixing ratios for other compounds tended to be of the same order of magnitude (e.g. m/z 101.059 (0.024 ± 0.021 ppb in this study, in which this compound is seen to be emitted) as that reported by Loubet et al. (2022) (0.02 [0.003–0.05] ppb) in which it is seen to be deposited. This explanation can, therefore, not be satisfactory, and another hypothesis that can be advanced is that the rapeseed crop has a closed-canopy structure, more critical than that of winter wheat crops, which would prevent methanol and other soluble BVOCs from being absorbed in soil solution.

4.2 BVOC daily emission and deposition flux dynamics

All BVOCs in this study exhibited diel emission or deposition patterns, with emission or deposition peaks around mid-day. Previous studies also reported these observations for all ecosystem types, confirming the close links between temperature and radiation with BVOC emissions and depositions (Guenther et al., 1995).

As has been reported earlier in many studies (Brilli et al., 2014; Gomez et al., 2021; Harley et al., 2007; Hüve et al., 2007; Mozaffar et al., 2017, 2018), methanol emissions during fruit development (P1) and early senescence (P2), and acetic acid (m/z 61.029) and m/z (63.006 + 63.026) during bare soil period (P4), exhibited an emission burst in the morning, before the radiation and temperature reached their maximums. During P1, as CO_2 fluxes also peaked earlier than noon, this could mean that the flux was mainly through stomata. However, during P2, this link was less clear, as CO_2 fluxes were small and the peak was of reduced magnitude. While emission bursts in the morning were also reported for other BVOCs like acetaldehyde and acetone in a poplar forest equipped with cuvettes (Brilli et al., 2014), this was not observed for these specific compounds in the present study.

4.3 Differences of BVOC emissions between cropping periods P1 to P4

In the present study, more significant emissions (SEF) of methanol, acetone, methanethiol and isoprene were observed during P3, at the end of the senescence period, compared to the two other vegetation periods, P1 and P2. Increased methanol, acetone and isoprene emissions during senescence have been recently put forward in wheat and maize (Bachy et al., 2018, 2020; Gomez et al., 2021; Gonzaga Gomez et al., 2019; Mozaffar et al., 2017, 2018), but to our knowledge, there is no information in the literature for rapeseed, as Havermann et al. (2022) investigated inflorescence emergence and flowering for this crop, but not senescence stages. These more significant emissions could result from the breakdown of cellular structures (Mozaffar et al., 2018; Rottenberger et al., 2005), a process analogous to those occurring during plant growth and cell wall expansion (Fall and Benson, 1996). However, we did not notice the same behaviour with monoterpenes (whose emissions were insignificant during P3). This decrease in monoterpenes emissions aligns with observations for rapeseed at

https://doi.org/10.5194/egusphere-2023-2438
Preprint. Discussion started: 9 January 2024

the plant scale by Gomez et al. (2021), who also observed a decrease in monoterpenes emissions as the plant entered senescence.

At the end of the senescence stage (P3), acetaldehyde was emitted, while the emission rates were insignificant in previous crop development stages. More significant emission rates of acetaldehyde during late senescence were also reported in wheat by Bachy et al. (2020). Graus et al. (2013), Gonzaga Gomez et al. (2019) and Bachy et al. (2016) observed bidirectional fluxes of acetaldehyde in maize, depending on the crop stage. Minimal formaldehyde emissions were also observed in the present study during late senescence. This BVOC was also reported by Gonzaga Gomez et al. (2019) in chamber measurements of rapeseed plants during the same measurement campaign as this study. However, such emissions were observed by Gonzaga Gomez et al. (2019) during the corresponding P1 period, when no significant eddy-covariance fluxes of formaldehyde were measured over that time. The more significant emissions observed in chambers by Gonzaga Gomez et al. (2019) may be attributed to higher temperatures in these devices. This compound's high OH reactivity (8.5' 10^{-12} cm^3 $molecule^{-1}$ s^{-1} at 298 K (IUPAC, 2023)) could also partly explain the low emission rates observed at the field scale with eddy covariance. Another possible explanation is that this compound has a proton affinity (712.9 $kJmol^{-1}$; NIST database, 2023) that is close to that of water (691 $kJmol^{-1}$; NIST database, 2023), potentially making it more difficult to detect it using the PTR-MS technique adequately.

During the bare soil period P4, fewer BVOCs were emitted; generally, the flux was lower than during the vegetated periods. In particular, methanol was emitted at its lowest rate, even if the order of magnitude was similar during all these periods (Table 1). Acetaldehyde (m/z 45.033), which was only emitted during P3 and P4, was emitted at a slightly larger rate than during senescence. The emission of acetaldehyde during the presence of leaf litter corroborates the observations made by Abis et al. (2021) in an experiment with rapeseed leaf litter. According to Seco et al. (2007), such acetaldehyde emissions could result from ozone exposure and leaf damage caused by sunlight. Bachy et al. (2016) also observed emissions of methanol and acetaldehyde over bare soil being in the same range as during vegetated periods. Bachy et al. (2016) and Schade and Custer (2004) report acetone emissions from crop soil, while we did not observe any significant emissions in this study.

According to our selection criteria (Section 2.4.2), no significant deposition flux was observed during the bare soil period. Acetic acid, a compound that Bachy et al. (2016) reported as predominantly deposited on bare soil compared to vegetation stages, was, on the contrary, only slightly emitted in the present study.

4.4 BVOC standard emission factors (SEF) and implication for modelling studies and OH reactivity

During periods P1 and P2, the methanol SEF was about 30 % of what is used in MEGAN2.1 (Guenther et al., 2012) and twice as Havermann et al. (2022) found. The SEF increased by roughly a factor of 4 from pre- to post-senescence (P2 to P3), which is larger than what was observed by Gomez et al. (2021) (SEF varying from about 1.1 to 1.3 $\mu g\ g^{-1}\ h^{-1}$). It is noticeable that in MEGAN2.1, the emission factor for bare soil (considered together with urban non-vegetated soils) is zero, principally lower than what we observed. Most noticeably, in our study, the SEF of isoprene and monoterpenes are much higher than what is used in MEGAN2.1: the isoprene SEF is 3 times larger, and the monoterpenes SEF is 2 to 30 times higher when the plant is active (before senescence). The SEF for sesquiterpenes is similar to what is reported in MEGAN2.1. Besides, our SEF during P1 and P2 for isoprene are 3 to 4 times smaller than in Gonzaga Gomez et al. (2019) and Havermann et al. (2022), while monoterpenes SEF are similar.

The present study therefore indicates that the contributions of monoterpenes to OH reactivity would be much underestimated by MEGAN2.1. The main contributors to OH reactivity in MEGAN2.1 are green leaf volatiles or stress VOC: indole and n-hexenal, which SEFs are 375 to 500 larger in MEGAN2.1 than in our study (Table 2). Guenther et al.

https://doi.org/10.5194/egusphere-2023-2438
Preprint. Discussion started: 9 January 2024

(2012) acknowledged the high degree of uncertainties for these compounds' emission factors due to the lack of measurements. We show in this study that these are likely small for oilseed rape, even after harvest. In this study, the OH reactivity constant of indole was taken from Atkinson et al. (1995), which was confirmed recently by Xue et al. (2022), giving some confidence in our calculations. Methanethiol and 4-oxopentanal also have SEFs 10 to 70 times larger in MEGAN2.1 (Table 2), leading to a significant contribution to OH reactivity. These are leaf surface VOC that are emitted by plant surface waxes when exposed to ozone or UVs (Fruekilde et al., 1998). We found in our study that for oilseed rape these compounds will not significantly contribute to the OH reactivity.

Despite the significant contribution of methanol to BVOC emissions in this rapeseed crop, its contribution to the total OH reactivity was relatively low, as also found by Bsaibes et al. (2020). Instead, rapeseed appeared to be a more significant emitter of terpenoids than previously reported and considered in the MEGAN.2.1 model. Since these compounds have a high reactivity in the atmosphere (OH reaction constants are about 100-fold larger for isoprene and monoterpenes than for methanol; Atkinson and Arey, 2003), they can largely contribute to total OH reactivity and impact air quality. Bsaibes et al. (2020) showed that isoprenoids contributed 40 % to the ambient OH reactivity over the same investigated field. Havermann et al. (2022) found terpenes contributed between 20 and 25 % of the BVOC emissions over the entire growing season.

As shown by Bsaibes et al. (2020), the contribution of this rapeseed crop to the amount of reactive species released in the atmosphere was low compared to forest ecosystems. However, in the present study, the total OH reactivity was about twice larger than what would be predicted by MEGAN2.1 if we remove contributions of indole, n-hexenal, methanethiol and 4-oxopentanal that seem to be primarily overestimated by the model. Since many compounds were not included in our calculations, the total OH reactivity is likely underestimated. Furthermore, we show that 85 % of that OH reactivity would be due to terpenoids while in MEGAN2.1, also after removing contributions from indole, n-hexenal, methanethiol and 4-oxopentanal, 80 % would be due to a combination of terpenoids (50 %), acetaldehyde (20 %) and methanol (10 %). This finding would have some implications for secondary organic aerosol formation as terpenoids and isoprenoids (isoprene, monoterpenes, sesquiterpenes) are more prone to produce SOA than methanol, acetone or acetaldehyde (Sakulyanontvittaya et al., 2008).

5 Conclusions

To our knowledge, this study is the first one to report BVOC fluxes measured by the eddy-covariance technique from a rapeseed field. This technique allowed us to quantify BVOC fluxes continuously at the field scale without disturbing the ecosystem. It showed that oxygenated BVOCs, and above all, methanol, are the main BVOCs emitted by this crop type. Notably, methanol contributed between 83% and 91% to the summed molar-based emission fluxes during vegetated and bare soil periods. As part of 53 compounds with significant fluxes, the other major emitted compounds were ethanol, monoterpenes, acetone, acetaldehyde and formaldehyde. Few compounds were seen to be deposited, among which formic and acetic acids were the most deposited. BVOC diel emission patterns were related to air temperature and solar radiation dynamics.

The standard emission factors computed in this study are based on a non-invasive method (eddy-covariance) and representative of the whole ecosystem. The methanol standard emission factor showed an increase in emissions by a factor of 4 during the late senescence stage, thereby confirming the necessity to use an ageing factor to represent methanol emissions in the model MEGAN2.1. Furthermore, the methanol standard emission factors appeared overestimated in MEGAN2.1 for the fruit development and start of senescence periods. Our study and recent literature also show that terpenoid standard emission factors should be increased for rapeseed in MEGAN2.1 by a factor between 3 and 90,

https://doi.org/10.5194/egusphere-2023-2438
Preprint. Discussion started: 9 January 2024

depending on the chemical species. These new emission factors would substantially modify the OH-reactivity profile from rapeseed, of which the contribution of terpenoids would be more critical than previously reported, therefore playing a significant role in SOA formation.

Author contribution

All co-authors contributed to this field campaign of the COV3ER project. PB analysed the data, initiated and wrote the manuscript with contributions of all co-authors, BL, RC, FL, CD and VG designed the field experiment. BD, OZ, JCG and OF carried out most of the technical work during the experiment, LGG performed BVOC chamber measurements during the field campaign, SB performed OH reactivity measurements during the field campaign, NZ thoroughly reviewed the manuscript.

Competing interests

The authors declare that they have no conflict of interest.

Data Availability

Meteorological and BVOC flux datasets can be found at https://doi.org/10.57745/AIINCW.

Acknowledgements

This study was supported by the region Île-de-France (DIM R2DS, Réseau francilien de Recherche sur le Développement Soutenable, project n° 1656), ADEME (COV3ER, project n°1562C0032) and the EU ICOS Research Infrastructure. The PTR-Qi-ToF-MS is a national instrument supported by ANAEE-FR services (ANR project n°11-INBS-0001). We gratefully thank Dominique Tristant, head of the AgroParisTech farm, for giving us access to his fields.

References

Abis, L., Kalalian, C., Lunardelli, B., Wang, T., Zhang, L., Chen, J., Perrier, S., Loubet, B., Ciuraru, R., and George, C.: Measurement report: Biogenic volatile organic compound emission profiles of rapeseed leaf litter and its secondary organic aerosol formation potential, Atmospheric Chemistry and Physics, 21, 12613–12629, https://doi.org/10.5194/acp-21-12613-2021, 2021.

AHDB, 2023, https://ahdb.org.uk/knowledge-library/the-growth-stages-of-oilseed-rape last consulted on 07/07/2023

Atkinson, R., Tuazon, E.C., Arey, J., and Aschmann, S.M.: Atmospheric and indoor chemistry of gas-phase indole, quinoline, and isoquinoline, Atmospheric Environment, 29(23), 3423-3432, 1995

Atkinson, R. and Arey, J.: Gas-phase tropospheric chemistry of biogenic volatile organic compounds: a review, Atmospheric Environment, 37, 197–219, https://doi.org/10.1016/S1352-2310(03)00391-1, 2003.

Aubinet, M., Grelle, A., Ibrom, A., Rannik, U., Moncrieff, J., Foken, T., Kowalski, A. S., Martin, P. H., Berbigier, P., Bernhofer, C., Clement, R., Elbers, J., Granier, A., Grunwald, T., Morgenstern, K., Pilegaard, K., Rebmann, C., Snijders, W., Valentini, R., and Vesala, T.: Estimates of the annual net carbon and water exchange of forests: The EUROFLUX methodology, Adv. Ecol. Res., 30, 113–175, 2000

Bachy, A., Aubinet, M., Schoon, N., Amelynck, C., Bodson, B., Moureaux, C., and Heinesch, B.: Are BVOC exchanges in agricultural ecosystems overestimated? Insights from fluxes measured in a maize field over a whole growing season, Atmos. Chem. Phys., 16, 5343–5356, https://doi.org/10.5194/acp-16-5343-2016, 2016.

https://doi.org/10.5194/egusphere-2023-2438
Preprint. Discussion started: 9 January 2024

Bachy, A., Aubinet, M., Amelynck, C., Schoon, N., Bodson, B., Moureaux, C., Delaplace, P., De Ligne, A., and Heinesch, B.: Methanol exchange dynamics between a temperate cropland soil and the atmosphere, Atmospheric Environment, 176, 229–239, https://doi.org/10.1016/j.atmosenv.2017.12.016, 2018.

Bachy, A., Aubinet, M., Amelynck, C., Schoon, N., Bodson, B., Delaplace, P., De Ligne, A., Digrado, A., du Jardin, P., Fauconnier, M.-L., Mozaffar, A., Müller, J.-F., and Heinesch, B.: Dynamics and mechanisms of volatile organic compound exchanges in a winter wheat field, Atmospheric Environment, 221, 117105, https://doi.org/10.1016/j.atmosenv.2019.117105, 2020.

Brilli, F., Gioli, B., Zona, D., Pallozzi, E., Zenone, T., Fratini, G., Calfapietra, C., Loreto, F., Janssens, I. A., and Ceulemans, R.: Simultaneous leaf- and ecosystem-level fluxes of volatile organic compounds from a poplar-based SRC plantation, Agricultural and Forest Meteorology, 187, 22–35, https://doi.org/10.1016/j.agrformet.2013.11.006, 2014.

Brilli, F., Gioli, B., Fares, S., Terenzio, Z., Zona, D., Gielen, B., Loreto, F., Janssens, I. A., and Ceulemans, R.: Rapid leaf development drives the seasonal pattern of volatile organic compound (VOC) fluxes in a 'coppiced' bioenergy poplar plantation: Seasonality of VOC fluxes in coppiced poplars, Plant, Cell & Environment, 39, 539–555, https://doi.org/10.1111/pce.12638, 2016.

Bsaibes, S., Gros, V., Truong, F., Boissard, C., Baisnée, D., Sarda-Esteve, R., Zannoni, N., Lafouge, F., Ciuraru, R., Buysse, P., Kammer, J., Gomez, L. G., and Loubet, B.: Characterization of Total OH Reactivity in a Rapeseed Field: Results from the COV3ER Experiment in April 2017, Atmosphere, 11, 261, https://doi.org/10.3390/atmos11030261, 2020.

Butcher, R. D., Macfarlane-Smith, W., Robertson, G. W., and Griffiths, D. W.: The identification of potential aeroallergen/irritant(s) from oilseed rape (*Brassica napus* spp. *oleifera*): volatile organic compounds emitted during flowering progression, Clinical & Experimental Allergy, 24, 1105–1114, https://doi.org/10.1111/j.1365-2222.1994.tb03315.x, 1994.

Butcher, R. D., Goodman, B. A., and Deighton, N.: Evaluation of the allergic/irritant potential of air pollutants: detection of proteins modified by volatile organic compounds from oilseed rape (Brassica napus ssp. oleiferd) using electrospray ionization-mass spectrometry, Clin Exp Allergy, 25, 985–992, https://doi.org/10.1111/j.1365-2222.1995.tb00401.x, 1995.

Courtois, E. A., Paine, C. E. T., Blandinieres, P.-A., Stien, D., Bessiere, J.-M., Houel, E., Baraloto, C., and Chave, J.: Diversity of the Volatile Organic Compounds Emitted by 55 Species of Tropical Trees: a Survey in French Guiana, J Chem Ecol, 35, 1349–1362, https://doi.org/10.1007/s10886-009-9718-1, 2009.

Das, M., Kang, D., Aneja, V. P., Lonneman, W., Cook, D. R., and Wesely, M. L.: Measurements of hydrocarbon air–surface exchange rates over maize, Atmospheric Environment, 37, 2269–2277, https://doi.org/10.1016/S1352-2310(03)00076-1, 2003.

Fall, R., and Benson, A.A.: Leaf methanol — the simplest natural product from plants. Trends Plant Sci. 1, 296–301. https://doi.org/10.1016/S1360-1385(96)88175-0, 1996

FAOSTAT 2023, https://www.fao.org/faostat/en/#home, last consulted 07/07/2023

Fruekilde, P., Hjorth, J., Jensen, N. R., Kotzias, D., and Larsen, B.: OZONOLYSIS AT VEGETATION SURFACES: A SOURCE OF ACETONE, 4-OXOPENTANAL, 6-METHYL-5-HEPTEN-2-ONE, AND GERANYL ACETONE IN THE TROPOSPHERE, Atmospheric Environment, 32(11), 1893-1902, 1998

Gallagher, M. W., Clayborough, R., Beswick, K. M., Hewitt, C. N., Owen, S., Moncrie, J., and Pilegaard, K.: Assessment of a relaxed eddy accumulation for measurements of #uxes of biogenic volatile organic compounds: study over arable crops and a mature beech forest, Atmospheric Environment, 13, 2000.

Gomez, L. G., Loubet, B., Lafouge, F., Ciuraru, R., Bsaibes, S., Kammer, J., Buysse, P., Durand, B., Gueudet, J.-C., Fanucci, O., Zurfluh, O., Decuq, C., Truong, F., Gros, V., and Boissard, C.: Effect of senescence on biogenic volatile organic compound fluxes in wheat plants, Atmospheric Environment, 266, 118665, https://doi.org/10.1016/j.atmosenv.2021.118665, 2021.

Gonzaga Gomez, L., Loubet, B., Lafouge, F., Ciuraru, R., Buysse, P., Durand, B., Gueudet, J.-C., Fanucci, O., Fortineau, A., Zurfluh, O., Decuq, C., Kammer, J., Duprix, P., Bsaibes, S., Truong, F., Gros, V., and Boissard, C.: Comparative study of biogenic volatile organic compounds fluxes by wheat, maize and rapeseed with dynamic chambers over a short period in northern France, Atmospheric Environment, 214, 116855, https://doi.org/10.1016/j.atmosenv.2019.116855, 2019.

https://doi.org/10.5194/egusphere-2023-2438
Preprint. Discussion started: 9 January 2024

Graus, M., Eller, A. S. D., Fall, R., Yuan, B., Qian, Y., Westra, P., de Gouw, J., and Warneke, C.: Biosphere-atmosphere exchange of volatile organic compounds over C4 biofuel crops, Atmospheric Environment, 66, 161–168, https://doi.org/10.1016/j.atmosenv.2011.12.042, 2013.

Gros, V., Zannoni, N.: Total OH Reactivity. In: Dulac, F., Sauvage, S., Hamonou, E. (eds) Atmospheric Chemistry in the Mediterranean Region. Springer, Cham., https://doi.org/10.1007/978-3-030-82385-6_7, 2022.

Guenther, A.: SEASONAL AND SPATIAL VARIATIONS IN NATURAL VOLATILE ORGANIC COMPOUND EMISSIONS, Ecological Applications, 7, 34–45, https://doi.org/10.1890/1051-0761(1997)007[0034:SASVIN]2.0.CO;2, 1997.

Guenther, A., Hewitt, C. N., Erickson, D., Fall, R., Geron, C., Graedel, T., Harley, P., Klinger, L., Lerdau, M., Mckay, W. A., Pierce, T., Scholes, B., Steinbrecher, R., Tallamraju, R., Taylor, J., and Zimmerman, P.: A global model of natural volatile organic compound emissions, J. Geophys. Res., 100, 8873, https://doi.org/10.1029/94JD02950, 1995.

Guenther, A. B., Jiang, X., Heald, C. L., Sakulyanontvittaya, T., Duhl, T., Emmons, L. K., and Wang, X.: The Model of Emissions of Gases and Aerosols from Nature version 2.1 (MEGAN2.1): an extended and updated framework for modeling biogenic emissions, Geosci. Model Dev., 5, 1471–1492, https://doi.org/10.5194/gmd-5-1471-2012, 2012.

Harley, P., Greenberg, J., Niinemets, U., and Guenther, A.: Environmental controls over methanol emission from leaves, 2007.

Havermann, F., Ghirardo, A., Schnitzler, J., Nendel, C., Hoffmann, M., Kraus, D., and Grote, R.: Modeling Intra- and Interannual Variability of BVOC Emissions From Maize, Oil-Seed Rape, and Ryegrass, J Adv Model Earth Syst, 14, https://doi.org/10.1029/2021MS002683, 2022.

Hüve, K., Christ, M., Kleist, E., Uerlings, R., Niinemets, Ü., Walter, A., and Wildt, J.: Simultaneous growth and emission measurements demonstrate an interactive control of methanol release by leaf expansion and stomata, Journal of Experimental Botany, 58, 1783–1793, https://doi.org/10.1093/jxb/erm038, 2007.

ICOS, 2021, ICOS Ecosystem Station Labeling report for station FR-Gri,

Isaksen, I. S. A., Granier, C., Myhre, G., Berntsen, T. K., Dalsøren, S. B., Gauss, M., Klimont, Z., Benestad, R., Bousquet, P., Collins, W., Cox, T., Eyring, V., Fowler, D., Fuzzi, S., Jöckel, P., Laj, P., Lohmann, U., Maione, M., Monks, P., Prevot, A. S. H., Raes, F., Richter, A., Rognerud, B., Schulz, M., Shindell, D., Stevenson, D. S., Storelvmo, T., Wang, W.-C., van Weele, M., Wild, M., and Wuebbles, D.: Atmospheric composition change: Climate–Chemistry interactions, Atmospheric Environment, 43, 5138–5192, https://doi.org/10.1016/j.atmosenv.2009.08.003, 2009.

IUPAC, 2023, IUPAC Task Group on Atmospheric Chemical Kinetic Data Evaluation – Data Sheet HOx_VOC11 (ipsl.fr)

Jakobsen, H.B., Friis, P., Nielsen, J.K., and Olsen, C.E.: Emission of volatiles from flowers and leaves of Brassica napus in situ, Phytochemistry, 37(3), 695-699, 1994

Kammer, J., Décuq, C., Baisnée, D., Ciuraru, R., Lafouge, F., Buysse, P., Bsaibes, S., Henderson, B., Cristescu, S. M., Benabdallah, R., Chandra, V., Durand, B., Fanucci, O., Petit, J.-E., Truong, F., Bonnaire, N., Sarda-Estève, R., Gros, V., and Loubet, B.: Characterization of particulate and gaseous pollutants from a French dairy and sheep farm, Science of The Total Environment, 712, 135598, https://doi.org/10.1016/j.scitotenv.2019.135598, 2020.

Kaplan, J. O., Folberth, G., and Hauglustaine, D. A.: Role of methane and biogenic volatile organic compound sources in late glacial and Holocene fluctuations of atmospheric methane concentrations: LATE GLACIAL AND HOLOCENE ATMOSPHERIC METHANE, Global Biogeochem. Cycles, 20, n/a-n/a, https://doi.org/10.1029/2005GB002590, 2006.

Karl, M., Guenther, A., Koble, R., Leip, A., and Seufert, G.: A new European plant-specific emission inventory of biogenic volatile organic compounds for use in atmospheric transport models, 29, 2009.

Karl, T., Guenther, A., Lindinger, C., Jordan, A., Fall, R., and Lindinger, W.: Eddy covariance measurements of oxygenated volatile organic compound fluxes from crop harvesting using a redesigned proton-transfer-reaction mass spectrometer, J. Geophys. Res., 106, 24157–24167, https://doi.org/10.1029/2000JD000112, 2001.

Kesselmeier, J., Bode, K., Gerlach, C., and Jork, E.-M.: Exchange of atmospheric formic and acetic acids with trees and crop plants under controlled chamber and purified air conditions, Atmospheric Environment, 32, 1765–1775, https://doi.org/10.1016/S1352-2310(97)00465-2, 1998.

https://doi.org/10.5194/egusphere-2023-2438
Preprint. Discussion started: 9 January 2024

Konig, G.: Relative contribution of oxygenated hydrocarbons to the total biogenic VOC emissions of selected mid-European agricultural and natural plant species, Atmospheric Environment, 29, 861–874, https://doi.org/10.1016/1352-2310(95)00026-U, 1995.

Langford, B., Acton, W., Ammann, C., Valach, A., and Nemitz, E.: Eddy-covariance data with low signal-to-noise ratio: time-lag determination, uncertainties and limit of detection, Atmos. Meas. Tech., 8, 4197–4213, https://doi.org/10.5194/amt-8-4197-2015, 2015.

Loubet, B., Laville, P., Lehuger, S., Larmanou, E., Fléchard, C., Mascher, N., Genermont, S., Roche, R., Ferrara, R. M., Stella, P., Personne, E., Durand, B., Decuq, C., Flura, D., Masson, S., Fanucci, O., Rampon, J.-N., Siemens, J., Kindler, R., Gabrielle, B., Schrumpf, M., and Cellier, P.: Carbon, nitrogen and Greenhouse gases budgets over a four years crop rotation in northern France, Plant Soil, 343, 109–137, https://doi.org/10.1007/s11104-011-0751-9, 2011.

Loubet, B., Buysse, P., Gonzaga-Gomez, L., Lafouge, F., Ciuraru, R., Decuq, C., Kammer, J., Bsaibes, S., Boissard, C., Durand, B., Gueudet, J.-C., Fanucci, O., Zurfluh, O., Abis, L., Zannoni, N., Truong, F., Baisnée, D., Sarda-Estève, R., Staudt, M., and Gros, V.: Volatile organic compound fluxes over a winter wheat field by PTR-Qi-TOF-MS and eddy covariance, Atmos. Chem. Phys., 22, 2817–2842, https://doi.org/10.5194/acp-22-2817-2022, 2022.

Mahilang, M., Deb, M. K., and Pervez, S.: Biogenic secondary organic aerosols: A review on formation mechanism, analytical challenges and environmental impacts, Chemosphere, 262, 127771, https://doi.org/10.1016/j.chemosphere.2020.127771, 2021.

Manco, A., Brilli, F., Famulari, D., Gasbarra, D., Gioli, B., Vitale, L., Tommasi, P. di, Loubet, B., Arena, C., and Magliulo, V.: Cross-correlations of Biogenic Volatile Organic Compounds (BVOC) emissions typify different phenological stages and stressful events in a Mediterranean Sorghum plantation, Agricultural and Forest Meteorology, 303, 108380, https://doi.org/10.1016/j.agrformet.2021.108380, 2021.

Mcewan and Macfarlane Smith: Identification of volatile organic compounds emitted in the field by oilseed rape (*Brassica napus* ssp. *oleifera*) over the growing season, Clinical & Experimental Allergy, 28, 332–338, https://doi.org/10.1046/j.1365-2222.1998.00234.x, 1998.

Morrison, E. C., Drewer, J., and Heal, M. R.: A comparison of isoprene and monoterpene emission rates from the perennial bioenergy crops short-rotation coppice willow and *Miscanthus* and the annual arable crops wheat and oilseed rape, GCB Bioenergy, 8, 211–225, https://doi.org/10.1111/gcbb.12257, 2016.

Mozaffar, A., Schoon, N., Digrado, A., Bachy, A., Delaplace, P., Du Jardin, P., Fauconnier, M.-L., Aubinet, M., Heinesch, B., and Amelynck, C.: Methanol emissions from maize: Ontogenetic dependence to varying light conditions and guttation as an additional factor constraining the flux, Atmospheric Environment, 152, 405–417, https://doi.org/10.1016/j.atmosenv.2016.12.041, 2017.

Mozaffar, A., Schoon, N., Bachy, A., Digrado, A., Heinesch, B., Aubinet, M., Fauconnier, M.-L., Delaplace, P., du Jardin, P., and Amelynck, C.: Biogenic volatile organic compound emissions from senescent maize leaves and a comparison with other leaf developmental stages, Atmospheric Environment, 176, 71–81, https://doi.org/10.1016/j.atmosenv.2017.12.020, 2018.

Müller, K., Pelzing, M., Gnauk, T., Kappe, A., Teichmann, U., Spindler, G., Haferkorn, S., Jahn, Y., and Herrmann, H.: Monoterpene emissions and carbonyl compound air concentrations during the blooming period of rape (Brassica napus), Chemosphere, 49, 1247–1256, https://doi.org/10.1016/S0045-6535(02)00610-0, 2002.

NIST database, 2023, https://webbook.nist.gov/chemistry/, last consulted 19/09/2023

Park, J.-H., Goldstein, A. H., Timkovsky, J., Fares, S., Weber, R., Karlik, J., and Holzinger, R.: Eddy covariance emission and deposition flux measurements using proton transfer reaction – time of flight – mass spectrometry (PTR-TOF-MS): comparison with PTR-MS measured vertical gradients and fluxes, Atmos. Chem. Phys., 13, 1439–1456, https://doi.org/10.5194/acp-13-1439-2013, 2013.

Park, J.-H., Fares, S., Weber, R., and Goldstein, A. H.: Biogenic volatile organic compound emissions during BEARPEX 2009 measured by eddy covariance and flux–gradient similarity methods, Atmos. Chem. Phys., 14, 231–244, https://doi.org/10.5194/acp-14-231-2014, 2014.

Peñuelas, J. and Staudt, M.: BVOCs and global change, Trends in Plant Science, 15, 133–144, https://doi.org/10.1016/j.tplants.2009.12.005, 2010.

https://doi.org/10.5194/egusphere-2023-2438
Preprint. Discussion started: 9 January 2024

Piesik, D., Pańka, D., Delaney, K. J., Skoczek, A., Lamparski, R., and Weaver, D. K.: Cereal crop volatile organic compound induction after mechanical injury, beetle herbivory (Oulema spp.), or fungal infection (Fusarium spp.), Journal of Plant Physiology, 168, 878–886, https://doi.org/10.1016/j.jplph.2010.11.010, 2011.

Ruuskanen, T. M., Müller, M., Schnitzhofer, R., Karl, T., Graus, M., Bamberger, I., Hörtnagl, L., Brilli, F., Wohlfahrt, G., and Hansel, A.: Eddy covariance VOC emission and deposition fluxes above grassland using PTR-TOF, Atmos. Chem. Phys., 11, 611–625, https://doi.org/10.5194/acp-11-611-2011, 2011.

Sakulyanontvittaya, T., Guenther, A., Helmig, D., Milford, J., and Wiedinmyer, C.: Secondary Organic Aerosol from Sesquiterpene and Monoterpene Emissions in the United States, Environ. Sci. Technol., 42, 8784–8790, https://doi.org/10.1021/es800817r, 2008.

Salazar Gómez, J.I, Klucken, C., Sojka, M., Masliuk, L., Lunkenbein, T., Schlögl, R., Ruland, H.: Elucidation of artefacts in proton transfer reaction time-of-flight mass spectrometers, J Mass Spectrom., 54, 987-1002, 2019

Sartelet, K. N., Couvidat, F., Seigneur, C., and Roustan, Y.: Impact of biogenic emissions on air quality over Europe and North America, Atmospheric Environment, 53, 131–141, https://doi.org/10.1016/j.atmosenv.2011.10.046, 2012.

Schade, G. W. and Custer, T. G.: OVOC emissions from agricultural soil in northern Germany during the 2003 European heat wave, Atmospheric Environment, 38, 6105–6114, https://doi.org/10.1016/j.atmosenv.2004.08.017, 2004.

Seco, R., Peñuelas, J., and Filella, I.: Short-chain oxygenated VOCs: Emission and uptake by plants and atmospheric sources, sinks, and concentrations, Atmospheric Environment, 41, 2477–2499, https://doi.org/10.1016/j.atmosenv.2006.11.029, 2007.

Sindelarova, K., Granier, C., Bouarar, I., Guenther, A., Tilmes, S., Stavrakou, T., Müller, J.-F., Kuhn, U., Stefani, P., and Knorr, W.: Global data set of biogenic VOC emissions calculated by the MEGAN model over the last 30 years, Atmos. Chem. Phys., 14, 9317–9341, https://doi.org/10.5194/acp-14-9317-2014, 2014.

Spirig, C., Neftel, A., Ammann, C., Dommen, J., Grabmer, W., Thielmann, A., Schaub, A., Beauchamp, J., Wisthaler, A., and Hansel, A.: Eddy covariance flux measurements of biogenic VOCs during ECHO 2003 using proton transfer reaction mass spectrometry, Atmos. Chem. Phys., 5, 465–481, https://doi.org/10.5194/acp-5-465-2005, 2005.

Stevenson, D. S., Zhao, A., Naik, V., O'Connor, F. M., Tilmes, S., Zeng, G., Murray, L. T., Collins, W. J., Griffiths, P. T., Shim, S., Horowitz, L. W., Sentman, L. T., and Emmons, L.: Trends in global tropospheric hydroxyl radical and methane lifetime since 1850 from AerChemMIP, Atmos. Chem. Phys., 20, 12905–12920, https://doi.org/10.5194/acp-20-12905-2020, 2020.

Sulzer, P., Hartungen, E., Hanel, G., Feil, S., Winkler, K., Mutschlechner, P., Haidacher, S., Schottkowsky, R., Gunsch, D., Seehauser, H., Striednig, M., Jürschik, S., Breiev, K., Lanza, M., Herbig, J., Märk, L., Märk, T. D., and Jordan, A.: A Proton Transfer Reaction-Quadrupole interface Time-Of-Flight Mass Spectrometer (PTR-QiTOF): High speed due to extreme sensitivity, International Journal of Mass Spectrometry, 368, 1–5, https://doi.org/10.1016/j.ijms.2014.05.004, 2014.

Veromann, E., Toome, M., Kännaste, A., Kaasik, R., Copolovici, L., Flink, J., Kovács, G., Narits, L., Luik, A., and Niinemets, Ü.: Effects of nitrogen fertilization on insect pests, their parasitoids, plant diseases and volatile organic compounds in Brassica napus, Crop Protection, 43, 79–88, https://doi.org/10.1016/j.cropro.2012.09.001, 2013.

Vivaldo, G., Masi, E., Taiti, C., Caldarelli, G., and Mancuso, S.: The network of plants volatile organic compounds, Sci Rep, 7, 11050, https://doi.org/10.1038/s41598-017-10975-x, 2017.

Vuolo, R. M., Loubet, B., Mascher, N., Gueudet, J.-C., Durand, B., Laville, P., Zurfluh, O., Ciuraru, R., Stella, P., and Trebs, I.: Nitrogen oxides and ozone fluxes from an oilseed-rape management cycle: the influence of cattle slurry application, Biogeosciences, 14, 2225–2244, https://doi.org/10.5194/bg-14-2225-2017, 2017.

Wiß, F., Ghirardo, A., Schnitzler, J.-P., Nendel, C., Augustin, J., Hoffmann, M., and Grote, R.: Net ecosystem fluxes and composition of biogenic volatile organic compounds over a maize field-interaction of meteorology and phenological stages, GCB Bioenergy, 9, 1627–1643, https://doi.org/10.1111/gcbb.12454, 2017.

Woźniak, E., Waszkowska, E., Zimny, T., Sowa, S., and Twardowski, T.: The Rapeseed Potential in Poland and Germany in the Context of Production, Legislation, and Intellectual Property Rights, Front. Plant Sci., 10, 1423, https://doi.org/10.3389/fpls.2019.01423, 2019.

https://doi.org/10.5194/egusphere-2023-2438
Preprint. Discussion started: 9 January 2024

Xue, J., Ma, F., Elm, J., Chen, J., and Xie, H.-B.: Atmospheric Oxidation Mechanism and Kinetics of Indole Initiated by ·OH and ·Cl: A Computational Study, Atmos. Chem. Phys., 22, 11543–11555, https://doi.org/10.5194/acp-22-11543-2022, 2022

Yáñez-Serrano, A. M., Filella, I., LLusià, J., Gargallo-Garriga, A., Granda, V., Bourtsoukidis, E., Williams, J., Seco, R., Cappellin, L., Werner, C., de Gouw, J., and Peñuelas, J.: GLOVOCS - Master compound assignment guide for proton transfer reaction mass spectrometry users, Atmospheric Environment, 244, 117929, https://doi.org/10.1016/j.atmosenv.2020.117929, 2021.